

2016

Electrophysiological properties of layer 5 pyramidal neurons in a mouse model of autism spectrum disorder

<https://hdl.handle.net/2144/17017>

"Downloaded from OpenBU. Boston University's institutional repository."

BOSTON UNIVERSITY
SCHOOL OF MEDICINE

Thesis

**ELECTROPHYSIOLOGICAL PROPERTIES OF LAYER 5
PYRAMIDAL NEURONS IN A MOUSE MODEL
OF AUTISM SPECTRUM DISORDER**

by

CARL SEILER HOLLAND III

B.A., Johns Hopkins University, 2013

Submitted in partial fulfillment of the
requirements for the degree of
Master of Science

2016

© 2016
CARL SEILER HOLLAND III
All rights reserved

Approved by

First Reader

Jennifer Luebke, Ph.D.
Associate Professor of Anatomy and Neurobiology

Second Reader

Maria Medalla, Ph.D.
Assistant Professor of Anatomy and Neurobiology

ACKNOWLEDGEMENTS

To my family. My Father, Mother, Brother and Grandparents. Thank you for your unwavering support and patience. I have been truly blessed with the most solid of roots. Without you, this, and all my success would not have been possible. I love you all.

To my friends. Both new and old. All I've had the pleasure to know. From Jacksonville, Baltimore, and Boston. I've been lucky to have y'all in my life.

To my lab mates and collaborators. Teresa Guillamon, Josh Gilman, Alex Hsu, Maya Woodbury, and Dr. Tsuneya Ikezu among others. Thank you for the support and the memories. I've had a wonderful time, due in no small part to your companionship and guidance. Thank you all.

To Dr. Maria Medulla. Your dedication to your work has been truly inspiring. Thank you for having the patience to listen to my endless stream of questions, and having the diligence to give me honest guidance in answering them. You have made lab both memorable and a constant learning experience.

To Dr. Jennifer Luebke. You have been, in all ways, an exemplary mentor. I cannot thank you enough for your support, knowledge, and guidance. Being in your lab has been a wonderful experience, both personally and professionally. I feel so very lucky to have had the privilege of working with you, and know what you have taught me will be a constant inspiration in my future career.

**ELECTROPHYSIOLOGICAL PROPERTIES OF LAYER 5
PYRAMIDAL NEURONS IN A MOUSE MODEL
OF AUTISM SPECTRUM DISORDER**

CARL SEILER HOLLAND III

ABSTRACT

Both neuroinflammation, and an increase in microglial cells, have been associated with Autism Spectrum Disorder (ASD) through observation in human subjects as well as in mouse models. A mother having an infection early in pregnancy increases the chances for autism in her child. (Atladottir *et al.*, 2012). This process is known as Maternal Immune Activation (MIA), and the proposed mechanism is that inflammatory signals cross from the mother to child; then in response to increased pro-inflammatory cytokines, microglia within the brain are activated to combat the infection. Microglia are essential to healthy synaptogenesis and neuronal growth, and a change in their signaling early in development has been shown to alter behavior in mouse models that replicate MIA. We use microglial depletion as a therapy to counteract the potentially harmful pro-inflammatory response in the developing mouse brain. Four experimental groups - control, MIA, microglial depleted, and a therapy group (MIA plus microglial depletion)- were run through a comprehensive series of behavioral and electrophysiological assessments. Layer 5 pyramidal cells (L5PNs) were targeted for recording in medial frontal cortex – a mouse cortical area important for cognition and social behavior. L5PNs are a heterogeneous population with cortical and subcortical targeting. Subcortical

targeting neurons are thick tufted morphologically, and have an intrinsically bursting spike pattern. Analysis of the intrinsically bursting neurons revealed significant differences between the maternal inflammation and the microglial depletion groups across multiple physiological properties. Therefore, the therapy group had electrophysiological characteristics more consistent with the microglial depleted model than the autism model.

TABLE OF CONTENTS

TITLE.....	i
COPYRIGHT PAGE.....	ii
READER APPROVAL PAGE	iii
ACKNOWLEDGEMENTS.....	iv
ABSTRACT.....	v
TABLE OF CONTENTS.....	vii
LIST OF TABLES.....	x
LIST OF FIGURES.....	xi
ABBREVIATIONS.....	xiii
INTRODUCTION.....	1
The Role of Microglia in Autism Spectrum Disorder	1
Creating a Profile of Maternal Immune Activation and Microglial Depletion.....	5
Classification of Layer 5 Pyramidal Neurons.....	7
Electrophysiological Properties of Layer 5 Pyramidal Neurons.....	10
MATERIALS AND METHODS.....	12
Experimental Subjects.....	12
Behavioral Studies.....	14

Preparation of Brain Slices for Recording and Filling.....	14
Cell Filling and Whole Cell Patch Clamp Recordings.....	15
Physiological Inclusion Criteria.....	15
Physiological Analysis.....	17
Slice Processing and Qualitative Assessment of Biocytin-filled neurons	18
Statistical Analysis.....	22
RESULTS.....	23
Layer 5 Pyramidal Neurons Demonstrate Multiple Electrophysiological Subtypes.....	23
Physiology of Regular Spiking Neurons.....	24
Physiology of Repetitive Oscillating Bursting Neurons.....	25
Synaptic Data for RS, IB, and ROB Neurons.....	32
Between Groups Data within the Intrinsically Bursting Pyramidal Neurons.....	36
Behavioral Data Between Groups.....	40
DISCUSSION.....	47
Electrophysiology of Experimental Groups.....	47
The Effect of Diversity of Layer 5 Pyramidal Neurons on this Study.....	49
Consistent Patterns of Differences in Electrophysiological and Behavioral Profiles.....	49

Conclusions	51
Future Directions.....	52
REFERENCES.....	54
CURRICULUM VITAE.....	58

LIST OF TABLES

Table	Title	Page
1	Experimental Groups.	13
2	Significant Differences of Electrophysiological Properties between Neurons of Different Firing Types.	27
3	Intrinsic Properties of Regular Spiking and ROB Neurons	31
4	Electrophysiological Properties of EPSCs and IPSCs	35
5	Between Groups ANOVAs.	37
6	Behavioral Data between Experimental Groups.	46

LIST OF FIGURES

Figure	Title	Page
1	Design of Maternal Immune Activation Experiment.	15
2	Slice Map Depicting Recordings of Layer 5 Cortex.	20
3	A Layer 5 Pyramidal Cell Filled with Biocytin.	21
4	Layer 5 Pyramidal Neuron Classes	26
5	Relative difference of Passive Properties between RS, IB, and ROB Neurons.	28
6	Relative difference of Active Properties between RS, IB, and ROB Neurons.	29
7	EPSC Properties of RS, IB and ROB Neurons	33
8	IPSC Properties of RS, IB and ROB Neurons	34
9	Tau Rn, and AP Duration at half of Intrinsically Bursting Cells by Group	38
10	Rheobase and Spike Number at +100 pA of Intrinsically Bursting Cells by Group	39

11	Hierarchical Clusters of Intrinsically Bursting Cells	41
12	Hierarchical Clusters of Intrinsically Bursting Cells Synaptic Properties	42
13	Hierarchical Clusters of Regular Firing Cells	43
14	Hierarchical Clusters of Regular Firing Cells Synaptic Properties	44

LIST OF ABBREVIATIONS

BU.....	Boston University
Amp.....	Single spike amplitude at peak
ANOVA.....	Analysis of Variance
AP.....	Action Potential
ASD.....	Autism Spectrum Disorder
Decay.....	Single spike decay time from peak to threshold
Dur $\frac{1}{2}$	Duration of action potential at one half amplitude
E9.5.....	Embryonic Day 9.5
EPSC.....	Excitatory Post Synaptic Current
HCA.....	Hierarchical cluster analysis
IB.....	Intrinsically Busting
IPSC.....	Inhibitory Post Synaptic Current
ISI.....	Inter Spike Interval
L5.....	Layer 5
L5PN.....	Layer 5 Pyramidal Neuron
LASC.....	Boston University Laboratory Animal Science Center
MIA.....	Maternal Immune Activation
P24.....	Day 24 post birth
PLX.....	PLX3397
Poly I:C.....	Polyinosinic:polycytidylic acid potassium salt

Post Hoc	Tukey's Post Hoc Test
Rise	Single spike Rise time from threshold to peak
ROB	Repetitive Oscillating Bursting
RS.....	Regular Spiking
Rn	Input Resistance
SD	Standard Deviation
SEM	Standard Error of the Mean
Tau	Membrane Time Constant
Vr	Resting Membrane Voltage

INTRODUCTION

The Role of Microglia in Autism Spectrum Disorder

Autism Spectrum Disorder (ASD) affects every 1 in 68 children born, and 3.5 million people total in the United States alone (CDC 2014). The symptoms of ASD include a host of behavioral deficiencies, mostly associated with social interaction. These symptoms exhibit a wide range of severity, which adds to the complexity of determining the mechanisms underlying this disorder. While some mechanisms have been characterized, others, like potential developmental and environmental factors, are still unknown. In order to make progress in combating ASD, new research must both characterize humans and animal models as well as develop novel therapies.

ASD is a heterogeneous neuronal disorder defined not by specific genetic or anatomical abnormalities, but by a triad of behavioral profiles. For an individual to be diagnosed with ASD, they must exhibit abnormal social interaction, have communication defects, and display repetitive behaviors (American Psychiatric Association, 1994). Because of such a broad definition, ASD includes a large host of disorders such as Aspergers syndrome and autistic disorder. The etiology of ASD is unclear. Having a genetic syndrome as the cause of ASD only accounts for about 15% of cases (Rossignol *et al.*, 2012). Using these disorders researchers have correlated ASD with defects in signaling, transcription, methylation, and neurotrophic genes (Silverman *et al.*, 2010).

However, how these genetic factors manifest into a social disorder is still poorly understood, especially when considering that ASD cases have such a wide range of social and intellectual capabilities (Pellicano *et al.*, 2006). Furthermore, causes of autism outside of genetic syndromes are even more variable. There is a high heritability associated with ASD. Monozygotic twins reaches a 90% concordance for ASD, while dizygotic twins have less than 10 % concordance, implying that genetic factors can play a large role (Silverman *et al.*, 2010). Therefore, researchers have developed a pool of at risk genes that increase the chances of developing the disorder.

Genetic abnormalities are not the only causes of ASD. ASD has also been associated with multiple environmental and developmental factors that likely lead to physiological abnormalities. The most prevalent abnormalities associated with ASD are immune dysregulation, inflammation, oxidative stress, mitochondrial dysfunction, and environmental toxicant exposure (Rossignol *et al.*, 2012). These physiological variables are the basis for the vast majority of mouse models used to study ASD. By replicating these abnormalities in mice, researchers are able to assess the potential effects of each variable on brain structure and function (Silverman *et al.*, 2010).

Postmortem human brains have been examined in order to create a neuroanatomical profile of ASD (Ashwood *et al.*, 2011). One of the major distinctions from a healthy brain is signs of neuroinflammation. More specifically, pro-inflammatory cytokines have been found in increased levels in the plasma and grey matter of ASD (Ashwood *et al.*, 2011). Research has linked maternal infection, which could make the fetus vulnerable to the mother's activated immune system releasing cytokines in the first

trimester, with a higher risk of the fetus developing ASD (Altadottir *et al.*, 2010). Because of results like these, one of the most prominent hypotheses in ASD research is that maternal immune system activation (MIA) can lead to ASD symptoms. However the signaling pathways and the underlying mechanisms of pro-inflammatory responses in ASD profile are still being researched. Along with signs of neuroinflammation, PET scans have demonstrated an increase in activated microglia within ASD patients in multiple areas of the brain (Suzuki *et al.*, 2013). Microglia are the primary macrophages of the central nervous system, and play a major role in immune defense as well as synaptogenesis. In the MIA hypothesis, it is proposed that the maternal infection prematurely activates microglia in the developing cortex of the fetus, and that aberrant activation continues in the cortex later in development and into childhood as well.

Microglial signaling has thus been a key focus of ASD research. The role of these cells in synaptogenesis and synaptic pruning is both essential to the repair and growth of neurons, especially in early development (Petanjek *et al.* 2011). However, research in mouse models has shown the pro-inflammatory cytokines such as interleukin 8, interleukin 6, and Tumor Necrosis Factor α , that are secreted by activated microglia, play a primary role in altered synaptogenesis and neurogenesis (Chez *et al.* 2007; Garay *et al.* 2013). The complexity of microglia signaling is highlighted by the observation that it is essential to healthy development, but that, possibly when activated by infection, its altered behavior could lead to ASD pathology. These pathways are not fully understood, but studies have shown that mutations in microglial signaling pathways result in mice with an ASD profile (Zhan *et al.*, 2014).

In order to better understand Maternal Immune Activation, multiple mouse models have been developed. In one model, polyinosinic:polycytidylic acid (Poly I:C) is injected into the mother during pregnancy in order to replicate an immune response in the fetus. This injection is shown to elicit neuroanatomical abnormalities in the mice, as well as behavioral changes after birth (Malkova *et al.*, 2012). Malkova measured decreases in social behavior in mice injected with Poly I:C when compared to control, and these changes persisted into adulthood. Poly I:C injection leads to an overabundance of microglia in the cortex, which is concurrent with the profile observed in postmortem human ASD brains (Morgan *et al.*, 2010). Using this rodent model, insight into the electrophysiological and morphological changes due to an overabundance of microglia can be studied in more detail.

Microglia abnormalities have been observed in multiple lobes and layers of the postmortem autistic brain. However there are some areas that seem particularly affected. There have also been recent studies that have highlighted the importance of microglia signaling in somatosensory, motor and prefrontal cortex (Hustler *et al.*, 2010, Carper *et al.*, 2005). These studies measured changes in cortical thickness in ASD brains, and concluded that the temporal and frontal cortex were the most highly effected due to local enlargement. Within the cortex, genetic studies have shown that layer 5 has a high amount of genes that correlate with ASD (Wilsey *et al.* 2013). Cortical layer 5 is populated by pyramidal neurons that are the principal neurons that project to other cortical and subcortical areas (Oswald *et al.* 2013). Activated microglia in ASD cause pyramidal cells to have an abnormally high density of spines (Hustler *et al.* 2010) and

this can be caused by an overabundance of microglia in the cortex. Therefore a decrease in microglia, even after the poly I:C injection, could alleviate some of the microglia associated structural and signaling changes in pyramidal neurons.

There is evidence that neonatal microglia, even when depleted to a fraction of their normal density, will repopulate rapidly and reach normal levels within the cortex. Researchers have shown that depleting microglia after neuron loss can increase functionality in the hippocampus (Rice *et al.* 2015). Microglial depletion is a potential therapy to combat harmful neuroinflammation. When PLX3397, a CSF1R inhibitor, (PLX) was administered for 30 days, it eliminated 99% of the microglia in the cortex (Rice *et al.* 2015). This inhibitor was administered after a lesion was inflicted that would normally result in microglial activation and neuroinflammation. Another study eliminated microglia using the same method in the adult mice, which resulted in the CNS rapidly replenishing the microglia after the PLX treatment was stopped. The mice with replenished microglia did not exhibit significant deficits when compared with wild type mice (Monica *et al.* 2015).

Creating a Profile of Maternal Immune Activation and Microglial Depletion

In the Ikezu MIA project from which the data used in this thesis was collected, there exists a much larger series of experiments exploring and categorizing MIA and the potential therapy of microglial depletion. This study has 4 groups: control, MIA Poly I:C

treated mice, microglial depleted (PLX) treated mice, and a fourth group given PLX after receiving a Poly I:C injection.

Hypothetically, the mice given Poly I:C demonstrate ASD like behavior. Poly I:C elicits neuroinflammation and increased numbers of microglia in the cortex of developing mice (Soumiya et al., 2011). Poly I:C is a treatment meant to mimic MIA thought to be important in the pathogenesis of ASD. An overabundance of synapses is observed in cortical neurons with Poly: I:C injections which is similar to the altered synaptic profiles observed in post mortem ASD patients (Hustler et al., 2010). For these reasons Poly I:C injection is a good model for studying the role of microglia in the presence of neuroinflammation.

The mice given the PLX treatment lose 99% of their microglia approximately nine days after birth. While noted above that in an adult mouse brain, the temporary loss of microglia has a small effect, its role in synaptogenesis and synaptic pruning during the development of a juvenile could have more adverse effects. However, these studies using PLX do not report a behavioral phenotype unlike wild type mice (Monica *et al.* 2015).

A group of mice also received both the Poly I:C and the PLX treatments. In theory, the Prenatal Poly I:C has created an neuroinflammatory environment with an overabundance of microglia. Shortly after birth, the administration of PLX temporarily eliminated the microglia from the cortex, decreasing the neuroinflammatory response and potentially rescuing some of the loss of function observed in the MIA model. The mechanism for this model could have a similar results as the hippocampal study, where

after a pro-inflammatory response induced by a lesion in the cortex. PLX administration post lesion increased functionality compared to the control (Rice *et al.* 2015).

These different experimental groups have all undergone the same battery of behavioral tests that focus on repetitive behavior and social proficiency. These tests included the maternal homing test that observes the juvenile mouse's tendency to maintain body contact with its mother and littermates (Zhan *et al.*, 2014). A marble burying test that measures repetitive behavior (Malkova *et al.*, 2012). Also a self-grooming test, open field test, and a 3-chambered social interaction test were also administered. (Malkova *et al.*, 2012) The result of these tests will be a behavioral profile of these juvenile mice. While the effect of the Poly I:C and PLX on mouse behavior has been documented, the results of the combine treatment could provide insight into microglial depletions ability to counteract the effects of neuroinflammation.

Classification of Layer 5 Pyramidal Neurons

After the behavioral tests are completed, the juvenile mice were prepped in order to perform electrophysiological recordings on L5PNs in frontal cortices (FC), including the medial prelimbic, anterior cingulate and lateral frontal association cortices (Allen Brain Atlas, <http://mouse.brain-map.org/>). Garay shows that the mFC, along with the cingulate cortex, is heavily affected by MIA. (Garay *et al.*, 2013) L5 was specifically targeted because of the concentration of synaptic density in frontal, premotor and temporal cortices as well as genetic markers for ASD having a high association with L5

of the cortex. (Hustler *et al.*, 2010, Wisley *et al.*, 2013) Therefore, L5PNs were used for electrophysiological recordings as well as morphological analysis.

Layer 5 is located from 400- 700 micrometers from the pial surface in the primary visual cortex (Shai *et al.* 2015). Within L5 there is a heterogeneous population of pyramidal neurons. These neurons have overlapping electrophysiological and morphological properties. However, because L5 PNs carry output from the local circuit to distant cortical and subcortical targets, they have been subject to a wide array of research in an attempt to categorize them. L5 has been commonly split into layer 5a, which is closer to the pial surface, and layer 5b, deep to layer 5a, due to their anatomical differences. The majority of PNs in Layer 5a have a smaller soma and have thinner apical tufts than Layer 5b neurons. (Schubert *et al.*, 2006) Therefore, as a generalization, layer 5a is populated with slender tufted neurons that have cortical or striatal targets, and are called corticocortical (CC) or corticostriatal (CStr) pyramidal neurons. Layer 5b is populated with thick tufted neurons that have subcortical or thalamic targets, and are called corticospinal (CS) or corticothalamic (CTh) pyramidal neurons. However, this is an oversimplification that understates the true complexity of L5PN diversity. In order to properly assess the effect of Poly I:C and PLX on L5PNs, their normative properties must be understood.

Recording from a layer with so much diversity has the potential to increase standard error (SEM) if the pyramidal neurons are not properly classified because of the large range of baseline electrophysiological properties. Researchers use a wide range of methods in order to properly classify these neurons. Among these methods

immunohistochemical staining and retrograde tracers are commonly used to build reliable neuronal profiles.

Immunohistochemical staining uses the proteins of pyramidal neurons associated with certain genetic prodigy or axonal targeting in order to characterized the cells displaying these proteins. Antibodies were used in an attempt to subdivide target specific PNs in L5. The effectiveness of these antibodies were assessed by comparing them to retrograde labeled cells. (Tantirigama *et al.*, 1015, McKenna *et al.*, 2011, and Lai *et al.*, 2008) The purpose of these papers was to phenotype L5PNs based on specific markers. For example, in McKenna 2011, they focused on neurons expressing the transcription factor FezF2, and attempted to find a distinct phenotype among L5PNs within the cortex using this marker. However, this phenotype seems to be distributed among the entirety of the subtype population including both subcortical and corticocortical projections. More importantly, Tantirigama used two separate antigens in an immunoassay to help separate CSp and CTh from the CStr and CC projecting neurons. The antigen CTIP2 binds to both CSp and CTh, while the SatB2 antigen binds to CStr and CC. There seems to be very little, if any, co expression among these two groups. This lack of coexpression allows for the accurate staining of separate types of L5PNs without a retrograde tracer.

Retrograde tracers are also used to categorize L5PNs. Hattox and Nelson attempted to classify retrograde-labeled L5 PNs based on their electrophysiological and morphological properties in the somatosensory cortex (Hattox *et al.* 2007). They found that subcortical pathways have similar properties, while the CStr and CC likewise have similar properties. Morphologically speaking, the sub cortical pathways both have more

apical dendrites and longer dendritic shaft width than CC or CStr. Similar research was done in Oswald 2013, however in this paper the results were run through an unsupervised cluster analysis. Oswald recorded electrophysiological data and then did confocal microscopy in an attempt to phenotype these subtypes without use of the retrograde tracers. Doing an unsupervised cluster analysis (24 electrophysiological and morphological parameters) yielded two subgroups. One was comprised of the CSp and CTh, and the other was CStr and CC. Using the first 10 variables in a principle components analysis, Oswald and coworkers were able to account for 90% of the variance between these two subgroups. However, within subgroups the analysis could not accurately subdivide between the subcortical CSp and CTh, or the cortical CStr and CC (Oswald *et al.*, 2013).

Electrophysiological Properties of Layer 5 Pyramidal Neurons

Pyramidal neurons in L5 fall into two broad categories based on their axonal targets. There is substantial overlap in the electrophysiological and morphological qualities in different types of subcortical neurons, and likewise in different types of cortical and striatal targeting neurons (Oswald *et al.*, 2013; Oswald *et al.*, 2015). However, a defining characteristic of subcortical neurons is their ability to show intrinsically bursting (IB) firing patterns (Molnar *et al.*, 2006; Hattox *et al.*, 2007). It is important to note that the vast majority of L5PNs are capable of regular spiking (RS) firing patterns either at warmer temperatures or high voltage input, however CC and CStr

neurons are incapable of intrinsically bursting under normal recording conditions. (Hedrick 2011) Therefore, at room temperature, the RS and IB coexist, with IB firing patterns being strongly correlated with PNs with subcortical targets. When retrograde labeling is used in classification of the PNs, only those that target subcortically have the ability to burst. Therefore, while IB neurons are not a consistent marker for a specific neuron profile, an IB pattern is strongly associated with subcortical targeting neurons (Christophe *et al.*, 2005; Kasper *et al.*, 1994).

MATERIALS AND METHODS

Experimental Subjects

A total of 12 wild type mice from five litters were utilized in this study. The mice were sacrificed at 8 to 10 weeks of age for patch clamp recordings. The animals, C57Bl/6 mice, were procured from Jackson Labs, Bar Harbor, ME, and housed in the Boston University Laboratory Animal Science Center (LASC). Both the Jackson Labs and the LASC are accredited by the Association of Laboratory Animal Care.

The mice under study were divided into 4 groups to study the effects of PLX and Poly I:C. Maternal immune activation (MIA) was induced by Polyinosinic:polycytidylic acid potassium salt (Poly(I:C) (Santa Cruz, sc-202767) injected on day 9.5 of embryonic development (E9.5)(20mg/kg). For microglia depletion, mice were given PLX3397 (Plexxikon, Inc) in the chow from days 21 to 42 after birth (P21-P42). For the induction of the mouse model of ASD, the mice were split into 4 groups of 3 mice each. Saline no PLX is the control; this group will receive saline injection at E9.5 and receive no Plexxikon treatment. Poly(I:C) no PLX receives a Poly(I:C) injection at E9.5 to induce maternal inflammation, and no Plexxiikon treatment. Saline + PLX receives a saline injection at E9.5 and Plexxikon treatment that depletes microglia in the cortex. Poly(I:C) + PLX receives both the Poly(I:C) and PLX treatment (Table 1).

Table 1. Experimental Groups.

Cohort	Models	Drug	Administration	Hypothesized Phenotype
A	Maternal Immune Activation	Poly I:C	Injection E9.5	Autism, Neuroinflammation
B	Microglial Depletion	PLX	In chow P21-P42	Microglia depleted during early development
C	Wild Type	None	N/A	Normal behavior
D	MIA + MD	Poly I:C +PLX	Poly I:C Injection E9.5, PLX in chow P21-P42	Effect of reduced microglia on neuroinflammation

Behavioral Studies

Prior to entry into the study described in this thesis, social behavior tests were used to determine if the MIA mouse model could be associated with ASD behavior. All behavioral tests were performed by the same researcher (Maya Woodbury, Boston University Pharmacology PhD candidate) in an empty testing room. For all tests, animals were brought to the testing room and habituated for at least 30 minutes before the start of testing. The tests included: nest/maternal homing test, self-grooming test, marble-burying test, open field, and 3chamber social interaction test (Figure 1) (Malkova *et al.*, 2012).

Preparation of Brain Slices for Recording and Filling

Mice were fully anesthetized with isoflurane before decapitation with guillotine. The brain was immediately removed and placed into ice cold oxygenated Ringer's solution (concentrations, in mM: 26 NaHCO₃, 124 NaCl, 2 KCl, 10 Glucose, 2.5 CaCl, 1.3 MgCl₂; pH=7.4, chemicals from Fluka, NY). The frontal cortex was mounted on an agar gel slab and then sliced into 300 μm thick slices using a vibrating microtome in oxygenated ice cold Ringer's solution. The slices were transferred to room temperature Ringer's solution for at least an hour before use in patch clamp experiments. Slices were transferred to a submersion type recording chamber affixed to the stage of an IR-DRC Microscope (Micro Video Instruments, Avon, MA, USA) and were consistently superfused in oxygenated room temperature Ringer's solution throughout the patch clamp experiments.

MIA Experimental Design

Does postnatal microglial depletion and replenishment correct abnormal behavior, layer V spine density and neuronal activity in MIA Autism mouse model?

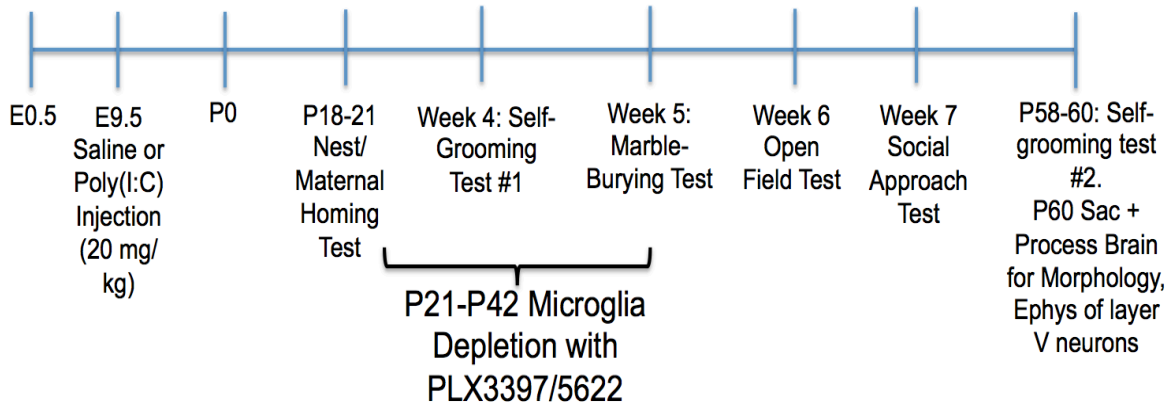


Figure 1. Design of Maternal Immune Activation Model. Depending on the experimental group, the mice will receive Poly I:C on E9.5, or PLX on days P21 to P42 in their chow. The order of behavior experiments through the study is also depicted until they are sacrificed for electrophysiological and morphological analysis. (Figure courtesy of Maya Woodbury, Ikezu Lab at Boston University School of Medicine Pharmacology Department)

Cell Filling and Whole Cell Patch Clamp Recordings

Slices were visualized under IR-DIC optics and a digital camera (Andor Xyla). L5PNs were identified by their distance from the pial surface of the cortex (400-700 μm). Electrodes were created from borosilicate glass and by a Flaming and Brown micropipette puller (Model P-87, Sutter Instruments, Novato, CA, USA). Pipettes were filled with a Potassium Methane Sulfonate internal solution (concentrations, in mM): 100 potassium methane sulfonate, 15 KCl, 3 MgCl₂, EGTA, 10 Na-HEPES, 1% biocytin (1% n-biotinyl-L-lysine), and had a resistance of 4-7 M Ω in external Ringer's solution. Standard whole cell patch clamp recording techniques (Amatrudo *et al.*, 2012) were used to examine the electrophysiological properties of these cells.

Physiological Inclusion Criteria

Cells were visually identified as L5 PN and were required to have stable access, low noise, and have a resting membrane potential below -55 mV in order to be used in the statistical analysis. The soma of L5 PN were located from 400 to 700 μm distant from the pial surface. Specific firing patterns that were associated with interneurons such as fast spiking or phasic spiking were also excluded. In order to include each neuron into the correct physiological group, the first inter-spike interval (ISI) of the first voltage step to induce a spike train was compared to the subsequent inter-spike intervals in the train. IB Neurons had a larger ISI compared to subsequent ISIs. RS Neurons had ISIs of the same length, or larger ISIs later in the spike trains (Schwindt *et al.*, 1997, Yang *et al.*, 1996).

Physiological Analysis

PatchMaster acquisition software on EPC-9 or EPC-10 patch-clamp amplifiers (HEKA Elektronik, Lambrecht, Germany) were used to acquire electrophysiological data including passive membrane properties, single action potential properties, and repetitive firing properties (Amatrudo *et al.*, 2012). 37 physiological characteristics acquired while recording. FitMaster Analysis Software was used in order to analysis passive and active membrane properties. The passive membrane properties, resting membrane potential (V_r), input resistance (R_n), and the membrane time constant (τ) were recorded using current clamp. V_r was measured while the current injection was at zero. R_n and τ were both measured by injecting 20 mV steps starting at -160 mV and ending at +100 mV. τ was measured by taking a stable trace with a small current injection (-20 or -40 mV) and recording the slope of the response of the membrane to the current injection. R_n was measured using a best fit line, each point representing the resistance at that 20 mV step, it is a function of the increase of voltage per current step (Ohm's Law).

Single spike properties (Threshold, Amplitude (Amp), Rise, Decay, and Duration at $\frac{1}{2}$ Amplitude (Dur $\frac{1}{2}$)) were measured from the first single spike recorded on the 200 ms current clamp. Threshold was measured at the point the action potentials slope was greater than one mV per millisecond. The amplitude was the maximum voltage recorded at the apex of the spike. Single spike rise was the time, in ms, for the action potential to rise from threshold to peak amplitude. Decay was the time for the action potential to

return to threshold from the peak amplitude. Dur $\frac{1}{2}$ is the duration of the spike from half amplitude on the rise to half amplitude on the decay of the spike.

Repetitive firing properties were measured in two separated traces, 2sHigh Rn trace and 2sLow Rn trace. The High Rn trace was a series of current clamp steps that increased by 20 mV from -100 mV to 120 mV. The Low Rn trace started at -170 mV and increased by 50 mV every step to 380 mV. The number of spikes per step was recorded.

In addition, the synaptic data was assessed using the Mini Analysis Program (Synaptosoft). The excitatory post synaptic currents (EPSCs) and inhibitory postsynaptic currents (IPSCs) that the program automatically detected were manually confirmed. Using the data of all the EPSCs or IPSCs gathered in a trace, an average waveform was created. From this we calculated average EPSC and IPSC Rise, Decay, Amplitude, Frequency and Area.

Slice Processing and Qualitative Assessment of Biocytin-filled neurons

Slices were fixed between pieces of filter paper in 4% paraformaldehyde in 0.1M phosphate buffered saline (PBS) at pH=7.4 immediately after recording. They were stored for 2 days at 4 degrees Celsius. At that point the slices were rinsed three times in PBS, put into a 1% Triton X-100/PBS solution for two hours at room temperature, then incubated in a streptavidin-Alexa 488 (1:500; InVitrogen, Carlsbad CA, USA) at 4 degrees Celsius for 2 days. For long term storage they were placed in a PBS Azide solution (.005% NaAzide in 01M PBS).

The location and morphology of biocytin-filled neurons recorded from were assessed using epi-fluorescence microscopy (Nikon and X-Cite Series 120Q fluorescent lamp). The overall quality of fills was assessed by amount of fluorescent background, brightness of the stain, and if the stain could be seen through the entirety of the dendritic arbors. Low magnification (4x) slice maps were imaged under IR-DIC and epi-fluorescence, using a digital camera (Andor Xyla) to verify the location and measure soma-to-pia distance of the recorded and filled cells in L5 (Figure 2).

A subset of biocytin filled neurons were further processed for immunohistochemistry for microglia-specific markers (P2ry12 and IBA1) and mounted on glass slides and coverslipped with Prolong anti-fade mounting medium (Invitogen), according to methods described in Medalla and Luebke (2015). These neurons were imaged in 3D using a Zeiss 710 confocal laser-scanning microscope with a 40x 1.3 N.A. oil-immersion lens and an Argon laser (Ex 488) as described previously (Amatrudo et al., 2012), for further detailed morphological analyses in a follow-up study (Figure 3).

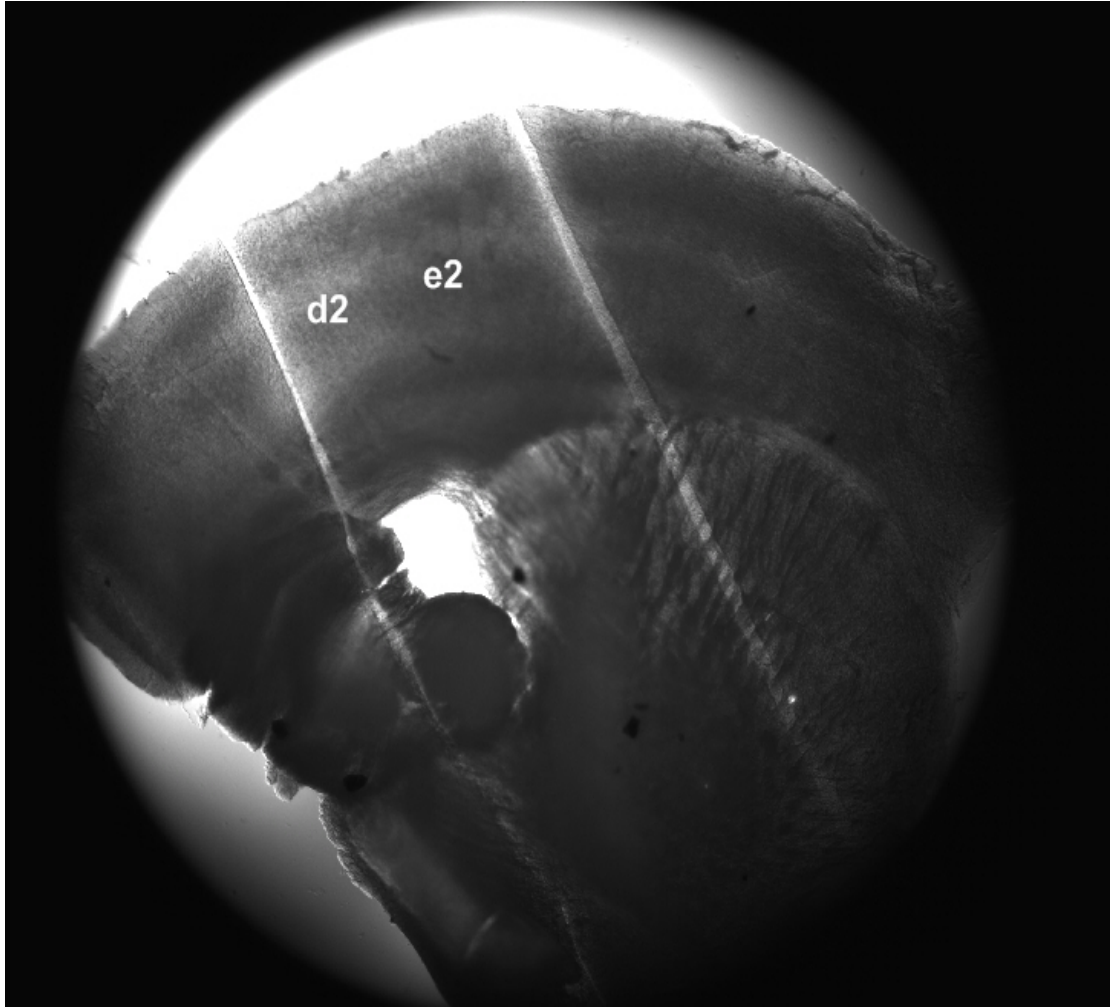


Figure 2. Slice Map Depicting Location of Recordings of PNs in Layer 5 of Cortex.

Two cells were recorded from in this slice. “d2” and “e2” were marked for confocal imaging. The cortical depth of the cells falls between 400 and 700 μm .

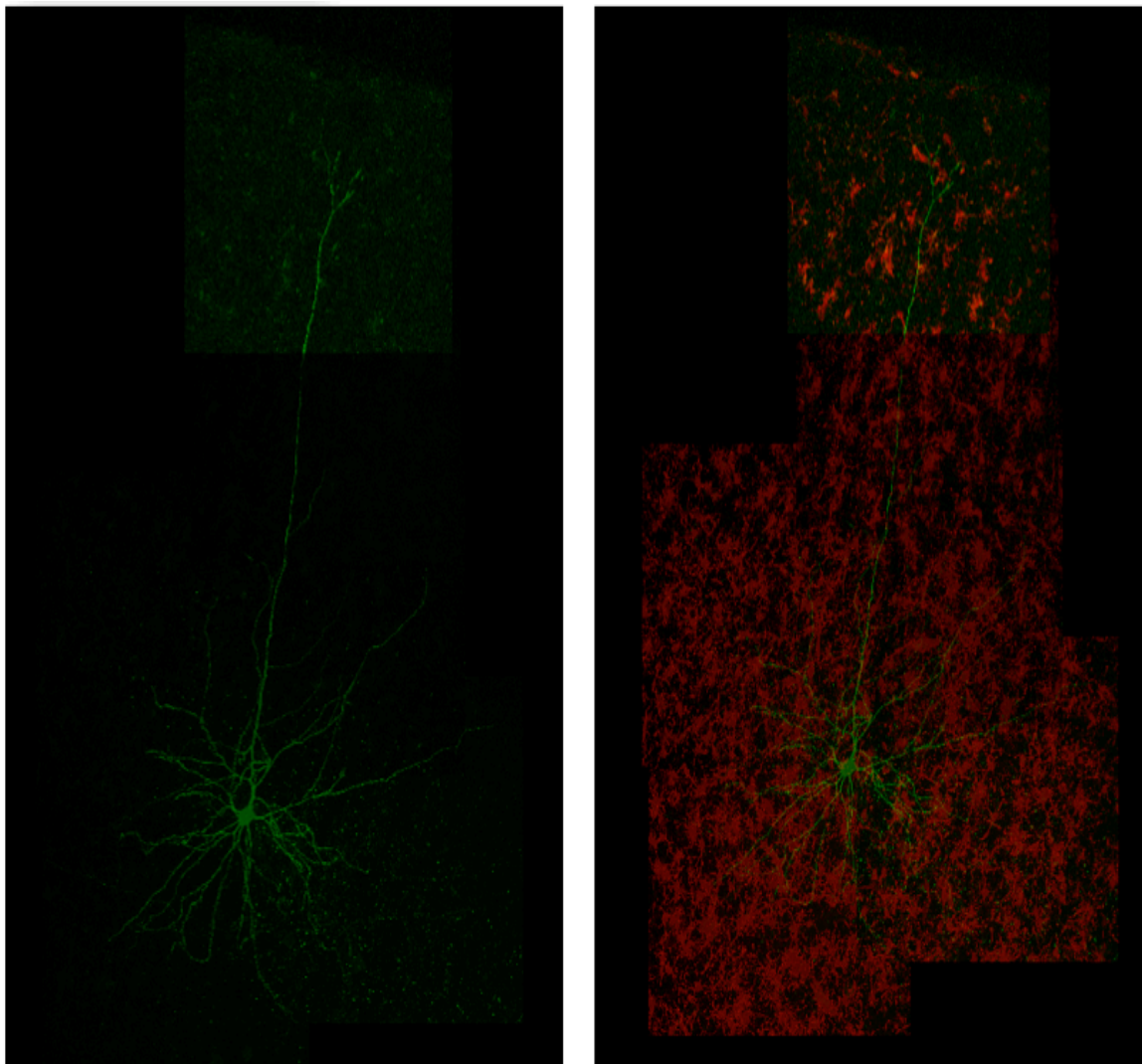


Figure 3. A Layer 5 Pyramidal Cell Filled with Biocytin. This is a confocal image of a L5PC. Notice the basal dendrites near the soma in L5, while the apical dendrite reaches towards the pial surface. The image on the left is the same neuron as on the right (green), but with the stain for P2ry12 and IBA1, which are proteins expressed in microglia (red).

Statistical Analysis

All data were compiled in a Microsoft Excel database, and for each variable measured, the mean, standard deviation and standard error of group was calculated. One-way ANOVA, with Fischer's LSD or Tukey's post-hoc tests were ran in SPSS in order to determine statistical differences between the 4 groups. To assess the relative proximity/similarity across the four groups based on multiple variables considered together, Hierarchical Cluster Analysis was run using SPSS. The HCA was run to cluster the four groups (and not the individual cells) using the means of each individual variable to create a proximity matrix based on pair-wise Euclidian distances. Significance of clustering within a similarity matrix was measured using The R Project for Statistical Computing.

RESULTS

Layer 5 Pyramidal Neurons Demonstrate Multiple Electrophysiological Subtypes

Of the 284 cells recorded from for this study, 215 neurons were classified as healthy L5 PNs based on their distance from pial surface (400 μm to 700 μm), repetitive firing properties, and having a stable resting potential of under -55 mV. Outliers were removed from the data by having at least five of their 37 recorded variables two standard deviations away from the average. Despite being passably healthy, these outliers either displayed firing properties associated with interneurons, such as fast or single spiking, or their physiology was deemed unacceptable due to poor access or to an insufficient seal between the electrode and the neuronal cell membrane.

Healthy L5 neurons were then categorized into RS (n= 140), IB (n= 61), and ROB (n=24) based on repetitive firing properties and ISI (Figure 4) (Hattox 2007). Student's T tests were used to determine if separating RS and IB neurons of the control group was a viable option for further analysis. To further confirm this preliminary analysis, an interactive ANOVA was run, comparing the experimental groups with the electrophysiological type. While there were few significant ANOVAs by group for electrophysiological properties, sorting by type had 7 different significantly different ANOVAs between the three subtypes, indicating that separation RS, ROB, and IB neurons is necessary (Figures 5 and 6).

In order to categorize a cell as intrinsically bursting or repetitive oscillation bursting, instead of regular spiking, certain criteria must be met. After determining that the cell is healthy and that the electrode has good access, the three steps that were used to determine firing type are the Two Second High Rn step (2sHigh), the Two second Low Rn Step (2sLow), and the RAMP. The 2sHigh (current step is 20 pA) and 2sLow (current step is 50 pA) maintained a consistent current injection for every step. The ramp increases one pA per millisecond. These protocols are used because they elicit action potential trains, and these repetitive firing properties are used to determine firing type. The cells recorded from are organized into three separate categories based of their repetitive firing properties.

Physiology of Regular Spiking Neurons

The profile of regular spiking cells (RS) was determined by the shape of a single action potential and the consistent inter-spike interval of the RS action potential trains. In the 2sHigh and 2sLow protocols, as the amount of current injected increases in each step, the RS neurons will have a consistent increase in spike number up until the point in which the neuron reaches the limit of its ability to fire action potentials. These spikes also have a consistent interval when measured from peak to peak. This peak-to-peak measurement is the inter spike interval (ISI). RS neurons in L5 tend to not have a large A current or depolarizing after potential. These currents were usually associated with IB neurons. However neurons whose spikes have these properties may still be regular firing

as long as these individual spike properties do not effect the aforementioned repetitive action potential properties. This current may elicit a doublet on the first action potential of a train, however this doublet does not indicate that the cell is bursting as long as it does not affect the ISI.

RS cells did not have any significant ANOVAs between groups. Even though the groups trended towards similar associations to IB cells between groups, as shown in the hierarchical clusters in figures 11 through 14 the large variation in their electrophysiological properties resulted in high standard error and a lack of significance despite having a very high number of cells (140 neurons). RS neurons have a significantly higher Rn ($p=.041$), slower Rise ($p=.01$), and larger Dur1/2 ($p=.03$) than IB neurons (Table 2).

Physiology of Repetitive Oscillating Bursting Neurons

The profile of Repetitive Oscillating Bursting neurons was determined a neurons ability to fire multiple bursts in any 2 second step (2sHigh, 2sLow) or R. Because IBs and ROBs have very similar bursting properties at higher current injections, lower current injections and the ramp were used to differentiate the two. This ability to fire multiple bursts in a single step is the only criterion for an ROB.

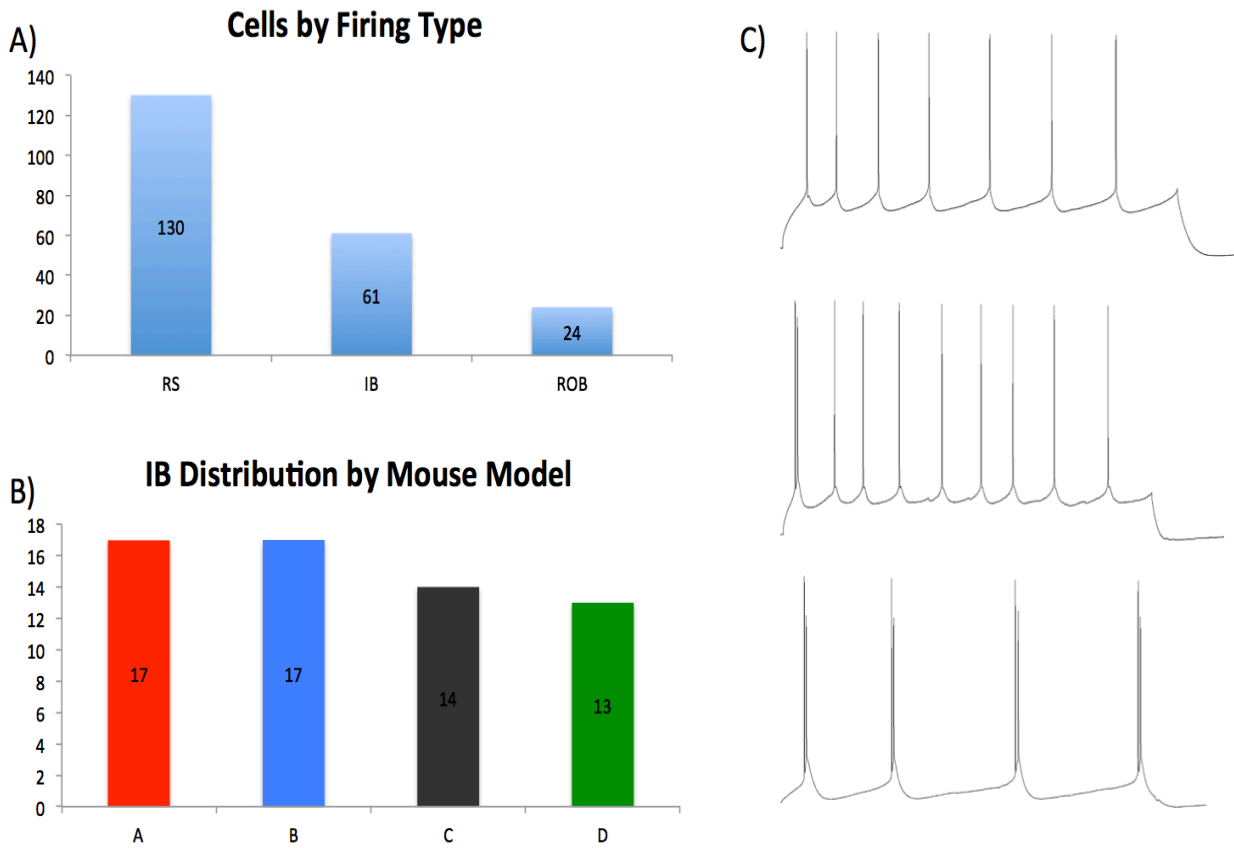


Fig 4. Layer 5 Pyramidal Neuron Classes A) Total $n = 215$, Regular Spiking Layer 5 Pyramidal Cells (RS) = 130, Intrinsically Bursting Layer 5 Pyramidal Cells (IB) = 61, and Rhythmic Oscillating Bursting Layer 5 Pyramidal Cells (ROB) = 24. B) The number of IB cells in each group. A = Maternal Inflammation; B = Microglial Depletion; C = Control; D = Maternal Inflammation and Microglial Depletion. C) Examples of the firing patterns of RS, IB, and ROB cells (from top to bottom).

Table 2. Significant Differences of Electrophysiological Properties between Neurons of Different Firing Types. Numbers in red are statically significant ($p > .05$) while numbers in blue are trending ($.05 < p < .1$). Note that the columns following “1 Way ANOVA” are Tukey’s Post Hocs showing the specific differences between groups.

	1 Way ANOVA	A vs B	A vs D	A vs C	C vs D
Tau	.051	.04	.039		
Rn	.034	.084	.039		
Rise	.01	.059	.009		
Decay	.032	.071	.047		
AP Dur 1/2	.012	.037	.016		
+40	.062	.044			
+100	.072	.16	.13	.13	
Rise EPSC	.025			.049	.035

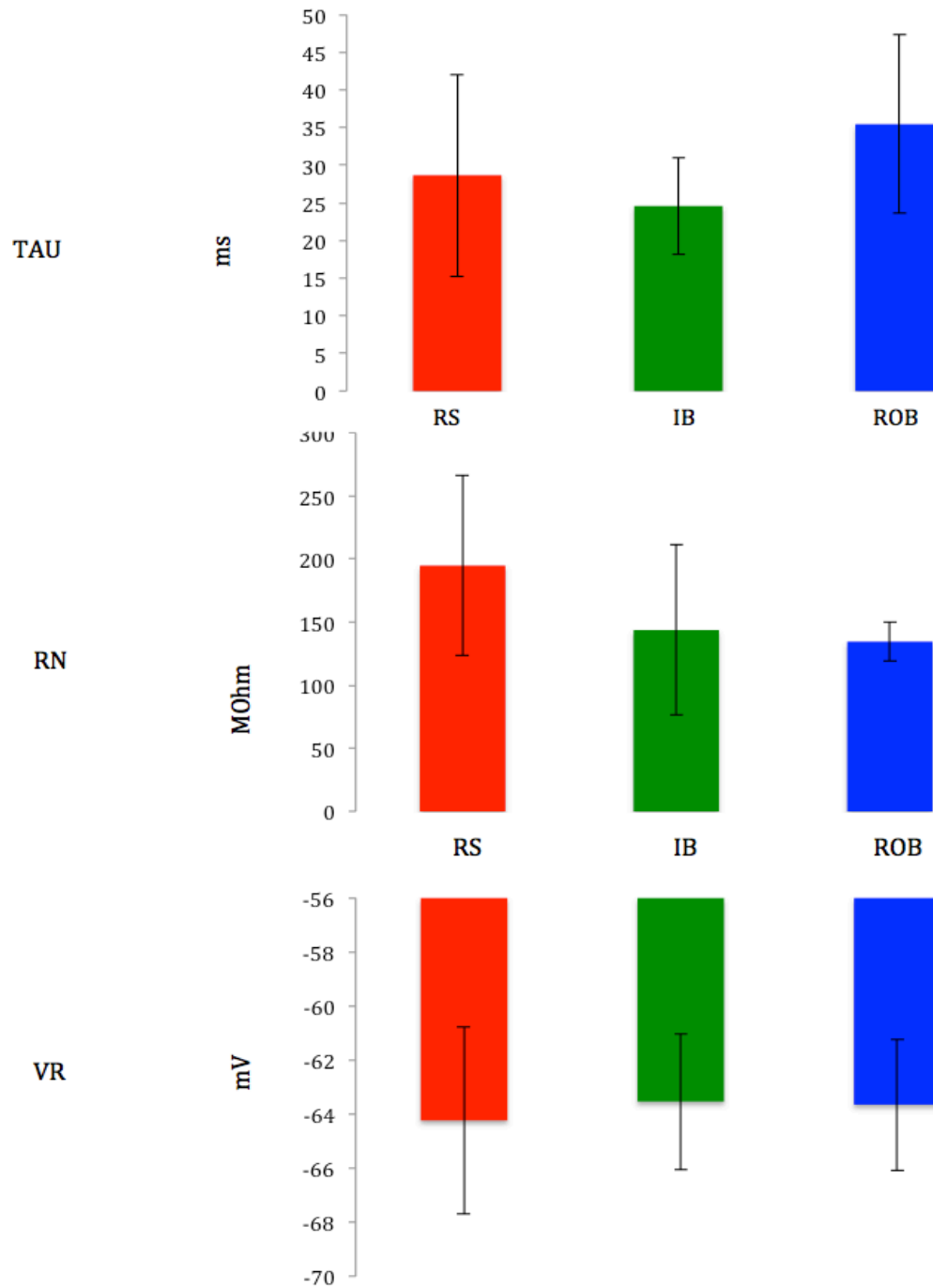


Figure 5. Relative difference of Passive Properties between RS, IB, and ROB

Neurons. Relative difference between RS (Red), IB (Green), and ROB (Blue) Neurons.

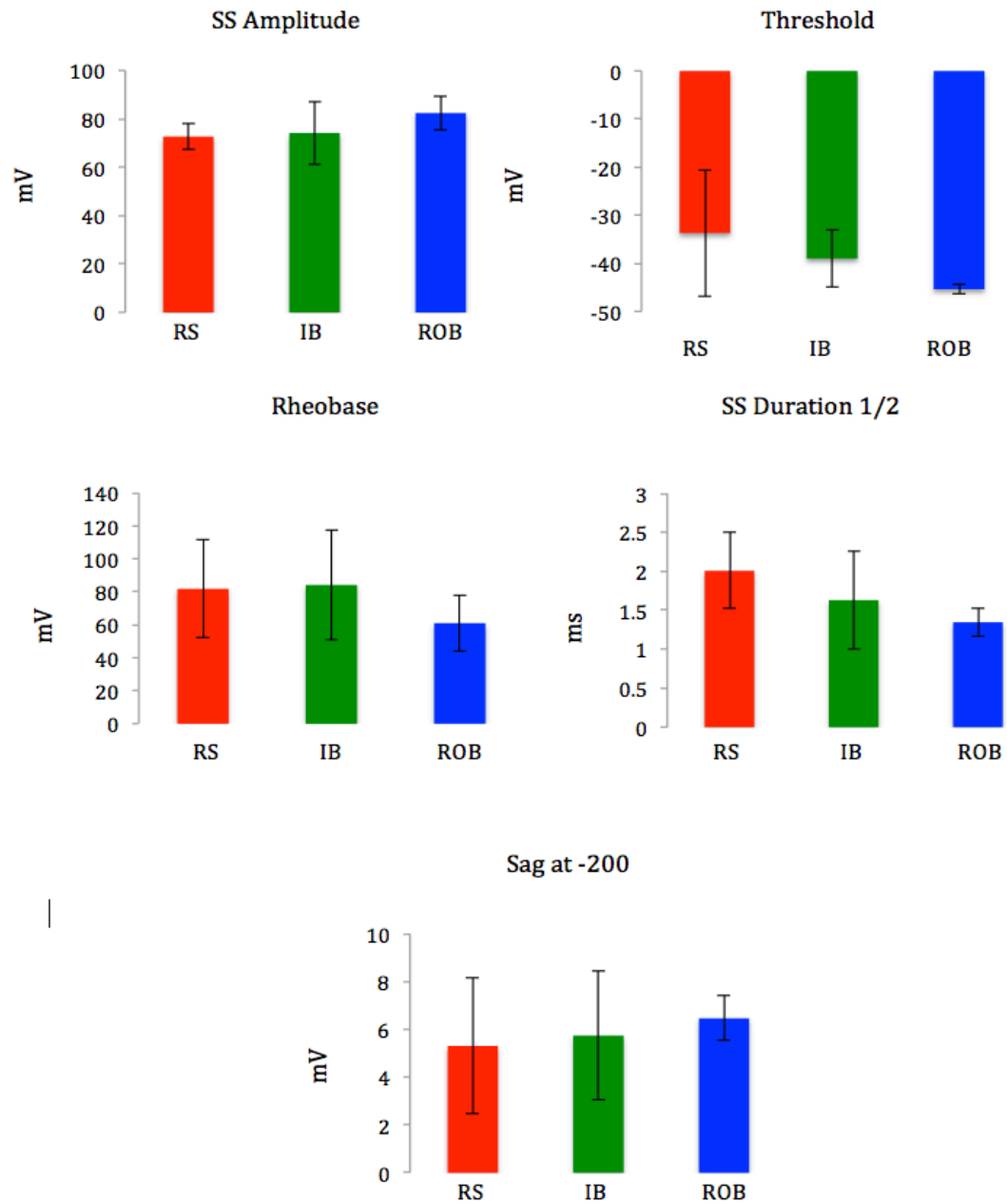


Figure 6. Relative difference of Active Firing Properties between RS, IB, and ROB Neurons. Relative difference between RS (Red), IB (Green), and ROB (Blue) Neurons.

ROB cells have a strikingly different electrophysiological profile when compared to IB and RS cells. However, due to a low number of cells it was determined that they were not a viable candidate for comparison across groups (Total n=24, control n=6). In the control group, T-tests confirmed that ROB cells had a significantly higher threshold (-45.38 mV) than both IB (-39.01 mV) and RS (-33.01 mV) neurons (Table 3). They also had a significantly lower Tau than IB neurons, but were otherwise similar. Compared to RS cells, ROB were significantly different in four of the five single spike measures (Threshold, Amplitude, Rise, and Duration at half Amplitude (Dur $\frac{1}{2}$) (Table 2). As the data implies, the bursting qualities of ROB neurons affect the shape of their action potentials.

Table 3. Intrinsic Properties of Regular Spiking and ROB Neurons

Regular Spiking

	Tau (ms)	Rn (MOhm)	Vr (mV) Threshld (mV)	Amp (pA)	Rise (ms)	Decay (ms)	Dur@1/2 (ms)	Sag @ -100	Sag @ -200	Abs Amp
A	Mean	176.70	-63.44	76.60	1.09	3.52	1.93	2.58	4.44	86.56
	SD	11.82	4.81	6.49	0.36	1.40	0.54	1.83	3.02	37.98
	n	40.00	40.00	40.00	40.00	40.00	40.00	40.00	40.00	40.00
B	Mean	26.73	-63.04	73.95	1.00	3.32	1.80	2.30	3.92	96.04
	SD	14.59	4.83	3.76	0.21	1.04	0.43	1.37	2.28	46.61
	n	28.00	28.00	28.00	28.00	28.00	28.00	28.00	28.00	28.00
C	Mean	28.67	-64.23	72.68	1.13	3.43	2.01	3.11	5.30	81.73
	SD	13.44	3.46	5.32	0.21	1.29	0.49	1.97	2.83	29.56
	n	40.00	40.00	40.00	40.00	40.00	40.00	40.00	40.00	40.00
D	Mean	27.26	-64.09	73.38	1.14	3.94	2.10	2.95	5.49	83.93
	SD	13.31	5.09	4.28	0.26	1.70	0.75	2.01	3.67	41.18
	n	22.00	22.00	22.00	22.00	22.00	22.00	22.00	22.00	22.00

ROB

	Tau (ms)	Rn (MOhm)	Vr (mV) Threshld (mV)	Amp (pA)	Rise (ms)	Decay (ms)	Dur@1/2 (ms)	Sag @ -100	Sag @ -200	Abs Amp
A	Mean	123.89	-60.86	80.95	0.76	2.13	1.24	2.71	5.72	74.20
	SD	11.63	3.02	4.77	0.09	0.40	0.15	1.30	1.68	21.95
	n	9.00	9.00	9.00	9.00	9.00	9.00	9.00	9.00	8.00
B	Mean	17.48	-16.28	31.57	3.28	3.85	3.46	4.34	5.13	35.05
	SD	12.48	38.72	42.81	4.96	4.55	4.82	4.10	3.20	34.52
	n	5.00	5.00	5.00	5.00	5.00	5.00	5.00	5.00	5.00
C	Mean	35.44	-63.65	82.40	0.81	2.43	1.35	3.31	6.46	60.97
	SD	11.83	2.43	6.99	0.15	0.75	0.18	0.52	0.94	17.00
	n	6.00	6.00	6.00	6.00	6.00	6.00	6.00	6.00	6.00
D	Mean	28.46	-59.44	80.75	0.83	2.60	1.40	3.44	6.54	76.72
	SD	13.79	2.69	5.89	0.07	0.60	0.11	1.08	1.09	12.95
	n	4.00	4.00	4.00	4.00	4.00	4.00	4.00	4.00	4.00

Synaptic Data for RS, IB, and ROB Neurons

The synaptic data between types of L5PNs uses the average waveform of all EPSC and IPSC events recorded over 120 seconds (Figures 5 and 6). High variation between individual subjects increases the SD of synaptic characteristics and therefore decreases their significance. For EPSCs the total number of cells per type in the control group was 10 for IB neurons, 15 for RS neurons, and 6 for ROB neurons (Table 4). For IPSCs the total number of cells per type in the control group was 10 for IB neurons, 15 for RS neurons, and 3 for ROB neurons. The low number of ROB neurons analyzed was due to a low initial count (n=6).

Within the EPSC data there was one significant ANOVA ($p=.013$) with the average amplitude of both IB and ROB neurons being significantly larger (Tukey's Post Hoc $p < .05$) than RS. Within the IPSC data there were two significant ANOVAs. In both amplitude ($p=.016$) and decay wave 37-90% ($p=.027$) RS was significantly different for ROB.

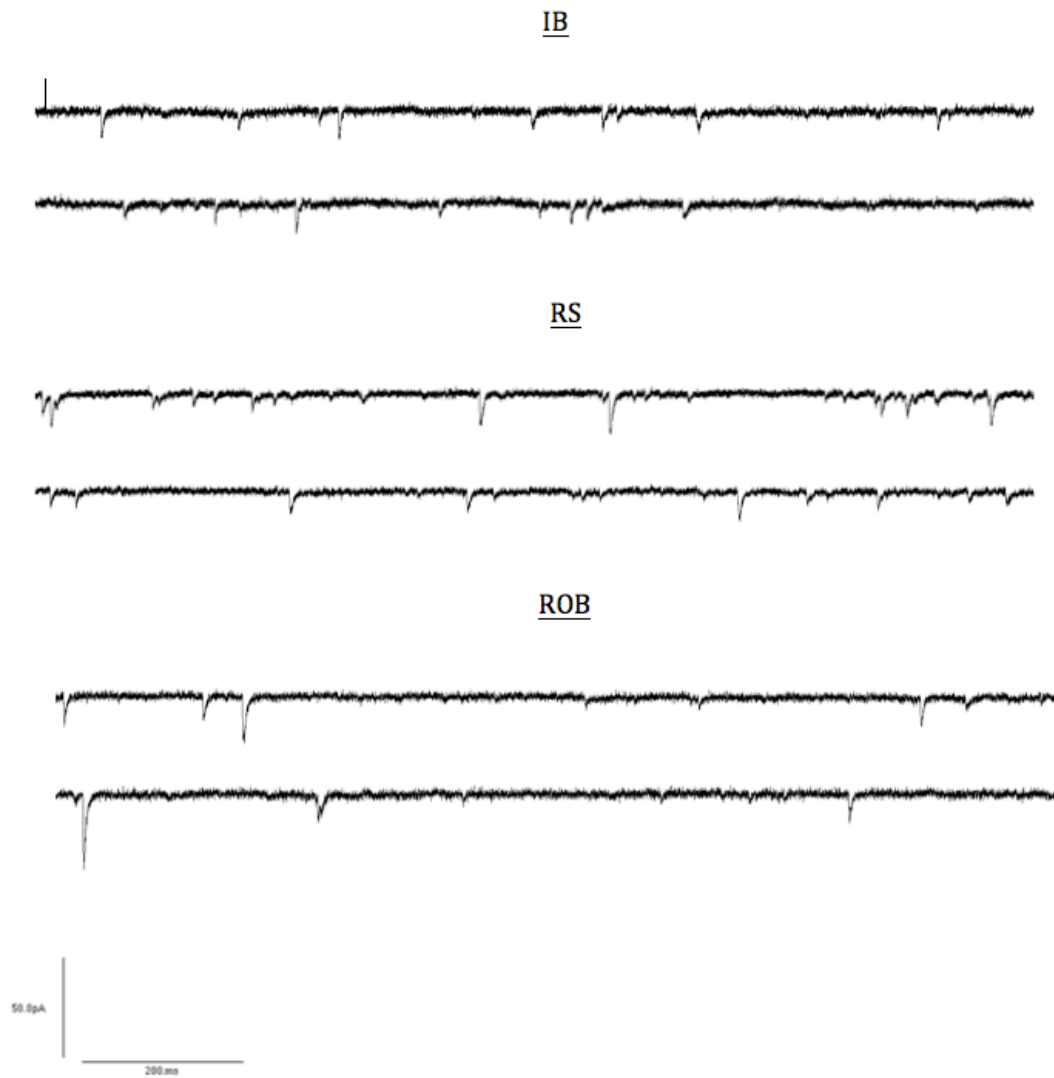


Figure 7. EPSC Properties of RS, IB and ROB Neurons. Traces were recorded from control cells being held at -80 mV.

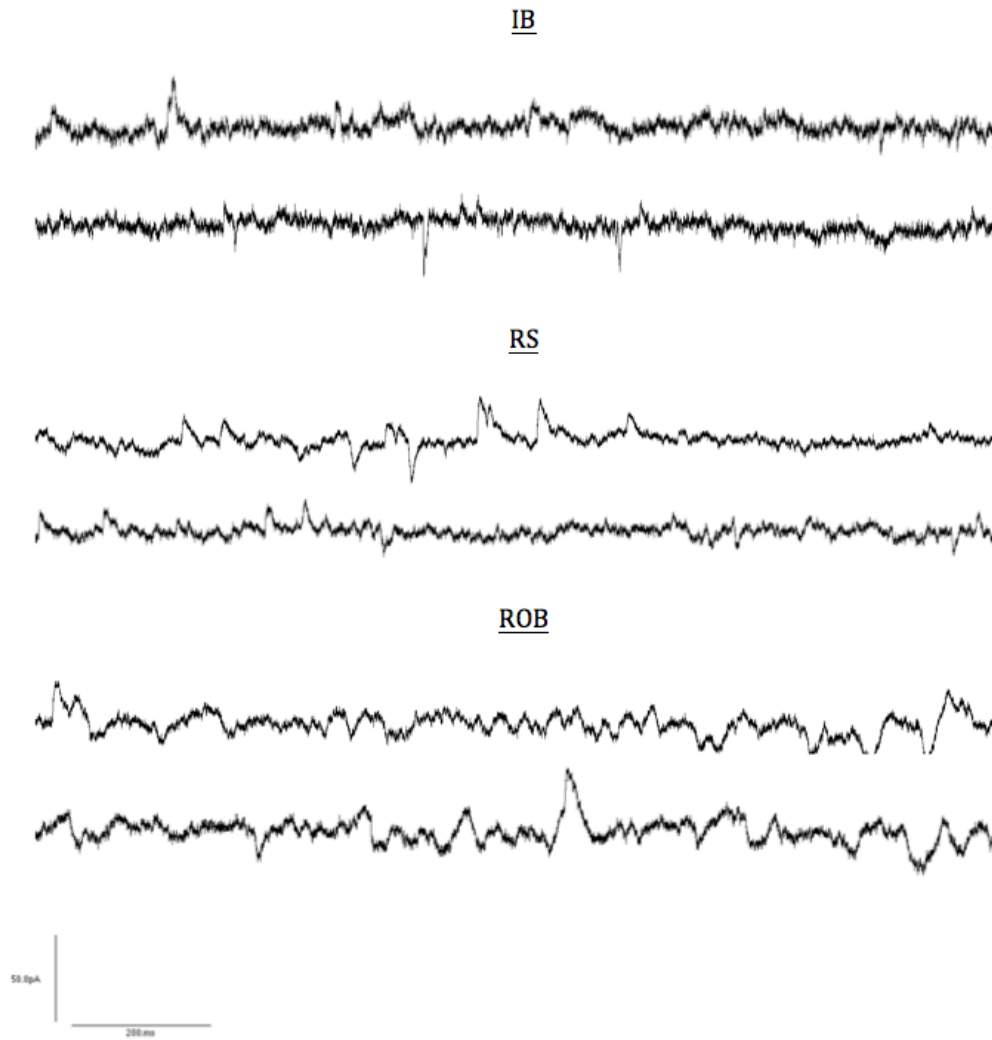


Figure 8. EPSC Properties of RS, IB and ROB Neurons. Traces were recorded from control cells being held at -40 mV.

Table 4. Electrophysiological Properties of EPSCs and IPSCs

EPSCs

	Frequency (Hz)	Amplitude (pA)	Rise (ms)	Decay (ms)	Area (pA/ms)	Decay 37-90%
IB	3.31+/1.35	21.06+/-9.08	2.94+/-0.42	4.89+/-0.96	100.29+/-66.43	5.19+/-0.75
RS	3.48+/-1.73	13.37+/-2.43	3.71+/-1.03	5.7+/-5.11	84.12+/-15.84	7.52+/-9.27
ROB	4.56+/-2.96	21.93+/-10.41	3.23+/-0.27	5.23+/-0.9	103.83+/-27.53	5.18+/-1.03

IPSCs

	Frequency (Hz)	Amplitude (pA)	Rise (ms)	Decay (ms)	Area (pA/ms)	Decay 37-90%
IB	0.32+/-0.34	60+/-42.36	6.56+/-1.46	11.17+/-2.88	792.15+/-662.42	9.59+/-3.13
RS	0.33+/-0.34	29.71+/-8.8	6.50+/-1.48	14.17+/-5.11	442.40+/-182.37	14.36+/-5.61
ROB	0.33+/-0.15	65.56+/-17.77	7.6+/-0.85	9.87+/-0.61	794+/-224.03	8.5+/-1

Between Groups Data for the Intrinsically Bursting Pyramidal Neurons

The profile of intrinsically bursting (IB) neurons was determined by the shape of a single action potential and a difference in the ISI of the IB repetitive firing properties. To qualify as IB, the initial action potential must be followed by an ISI that is larger than the subsequent interspike intervals in the train. Because this bursting activity eventually resembles the RS profile at higher current injections, lower steps in the 2sHigh and 2sLow, as well as the RAMP are used to determine if a cell is IB.

The IB group was used as a focus of the between experimental groups data. As seen in Table 5, there were five significant, $p < .05$, ANOVAs (Rn, Rise, Decay, Dur $\frac{1}{2}$, and rise EPSC) and three trending, $.05 < p < .1$ ANOVAs (Tau, +40, and +100 steps). The vast majority of the differences were between the Poly I:C group and the PLX group. In terms of post hocs, there were three significant post hocs between the Poly I:C and PLX groups, and three trending. The Poly I:C and the Poly I:C/ PLX group also had five significant post hocs between them. The control group was not significantly different from any of the other group except for in Rise EPSC (ANOVA= .025) where post hocs showed significant difference between the control and both the Poly I:C ($p = .049$) and Poly I:C/ PLX groups ($p = .035$).

Table 5: Between Groups ANOVAs. Numbers in red are statically significant ($p > .05$) while numbers in blue are trending ($.05 < p < .1$). Note that the columns following “1 Way ANOVA” are Tukey’s Post Hocs showing the specific differences between groups.

	1 Way ANOVA	A vs B	A vs D	A vs C	C vs D
Tau	.051	.04	.039		
Rn	.034	.084	.039		
Rise	.01	.059	.009		
Decay	.032	.071	.047		
AP Dur 1/2	.012	.037	.016		
+40	.062	.044			
+100	.072	.16	.13	.13	
Rise EPSC	.025			.049	.035

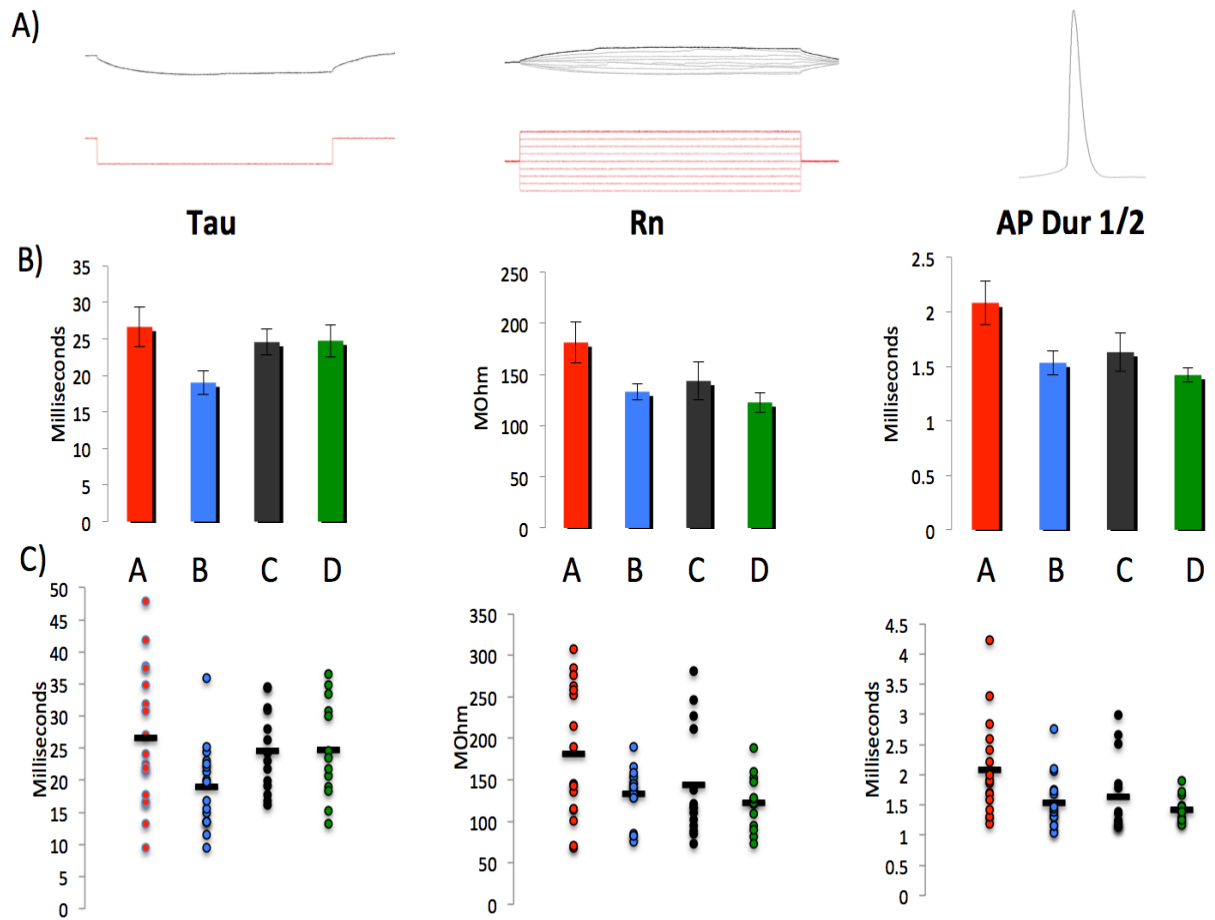


Fig 9. Tau Rn, and AP Duration at half of Intrinsically Bursting Cells by Group A)

Traces of raw data for each property (Tau, Rn, and Action Potential Duration at Half Amplitude). B) Bar graphs comparing the different groups by electrophysiological properties with error bars representing SEM. C) Parallel Dot Plots for each individual cell within each group. Horizontal bars in the middle of each plot indicate the mean value for that group.

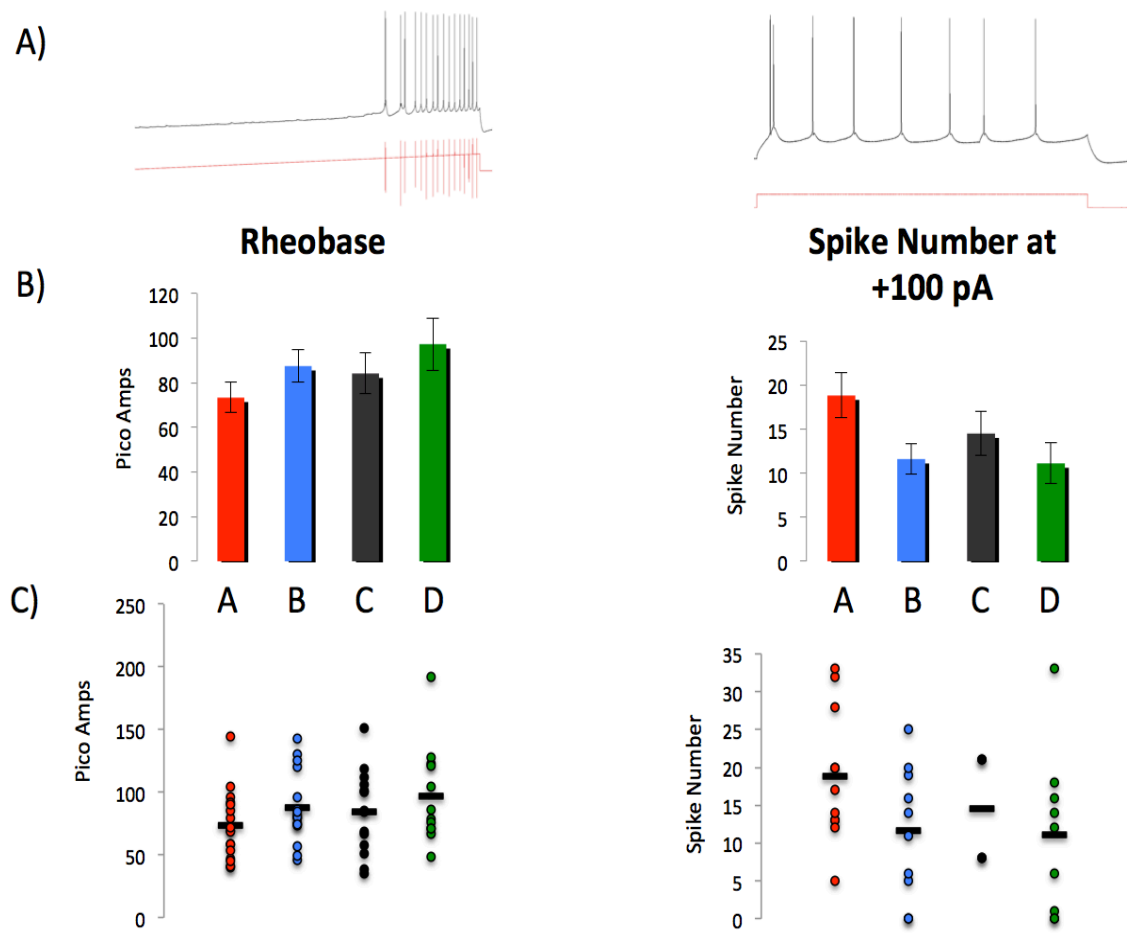
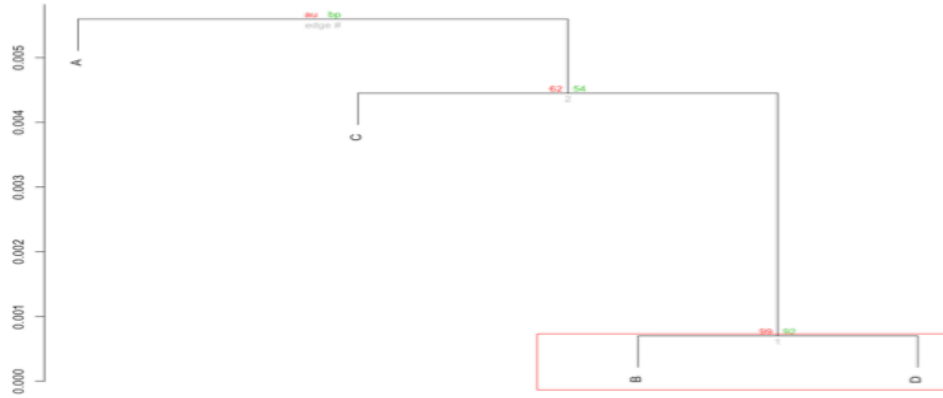


Figure 10. Rheobase and Spike Number at +100 pA of Intrinsically Bursting Cells by Group A) Traces of raw data for each property (Rheobase and Number of Spikes at a 100 mV trace over 2 seconds). B) Bar graphs comparing the different groups by electrophysiological properties with error bars representing SEM. C) Parallel Dot Plots for each individual cell within each group. Bars in the middle of each plot indicate the mean value for that group.

A high Rn usually correlates with faster single spike properties (Rise, Decay, and Dur ½) and a low Rheobase as is shown in Figure 10. The consistent post hocs also imply significance over multiple physiological characteristics (Figure 9 and Figure 10). In order to properly assess the hypothesis that the data was consistent, multiple hierarchical cluster analysis were run as shown in Figures 11 through 14. These figures show that the PLX and Poly I:C/ PLX groups clustered significantly in 7 of the 8 hierarchical clusters ($p < .05$, significant clustering is shown by the red box). Clusters use the means of a subset electrophysiological characteristics in order to derive a similarity matrix. The Euclidian distance is a measure of relative distance between the different groups. The smaller the distance, the more similar the groups were while using that subset of factors. Significance of the cluster is measured using the bootstrap method. The All Variables IB and RS clusters used 36 recorded electrophysiological characteristics. The Intrinsic IB and RS clusters used the 11 characteristics (Tau, Rn, Vr, Threshold, Rise, Decay, SS Amp, Dur ½, Sag -100, Sag -200 and Rheobase). The EPSC and IPSC clusters both used six variables (frequency, amplitude, rise, decay, area, decay 37-90%).

IB ALL VARIABLES



IB INTRINSIC PROPERTIES

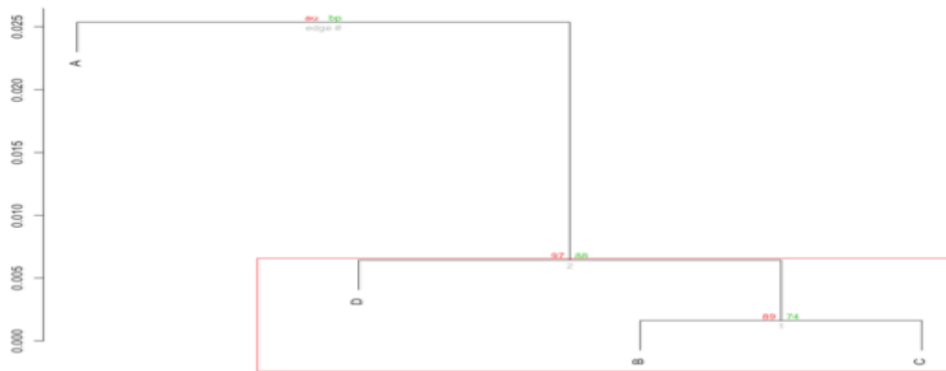
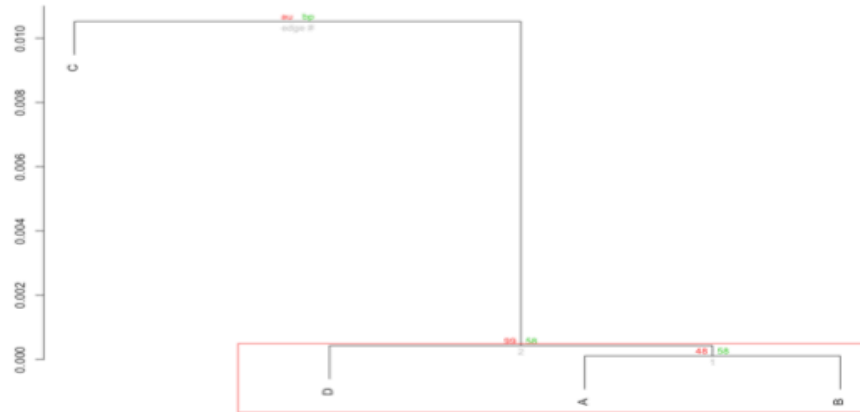


Figure 11. Hierarchical Clusters of Intrinsically Bursting Cells Dendrograms showing the Euclidian distance between the means of each electrophysiological property for groups A (Poly I:C), B (PLX), C (Wild Type), and D (Poly I:C and PLX). The smaller the squared Euclidian distance between groups, the more similar the groups are. For example, in the Hierarchical Cluster for “IB All Variables” 37 electrophysiological properties are used in order to measure the relative distance between the groups.

IB EPSC PROPERTIES



IB IPSC PROPERTIES

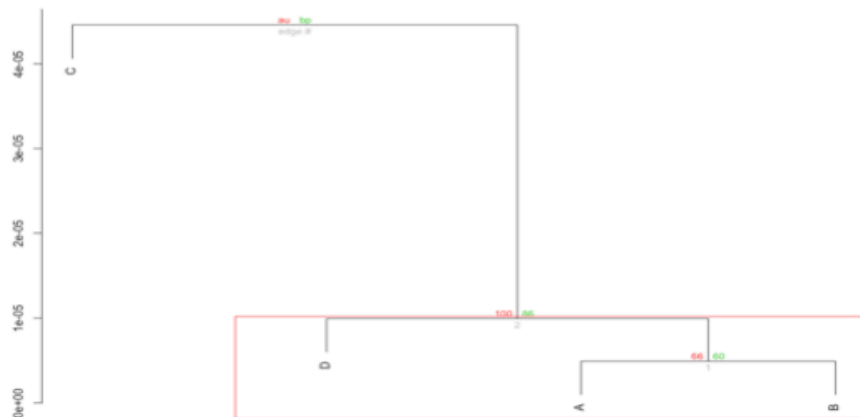
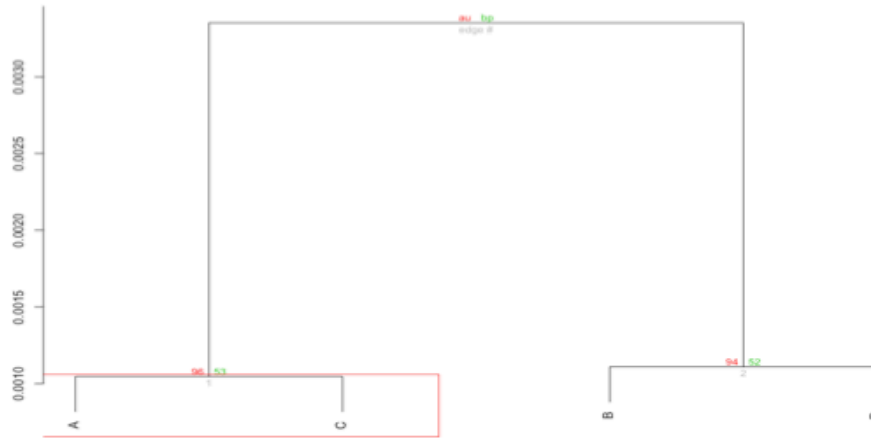


Figure 12. Hierarchical Clusters of Intrinsically Bursting Cells Synaptic Properties

Dendrograms showing the Euclidian distance between the means of each electrophysiological property for groups A (Poly I:C), B (PLX), C (Wild Type), and D (Poly I:C and PLX).

RS ALL VARIABLES



RS INTRINSIC PROPERTIES

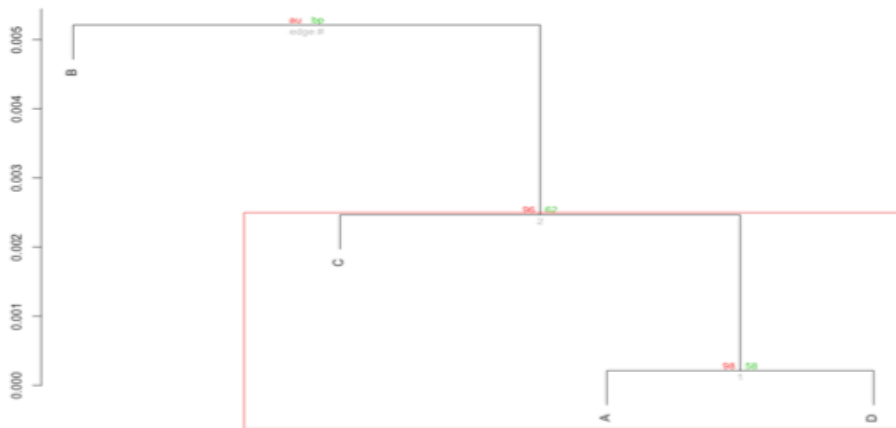
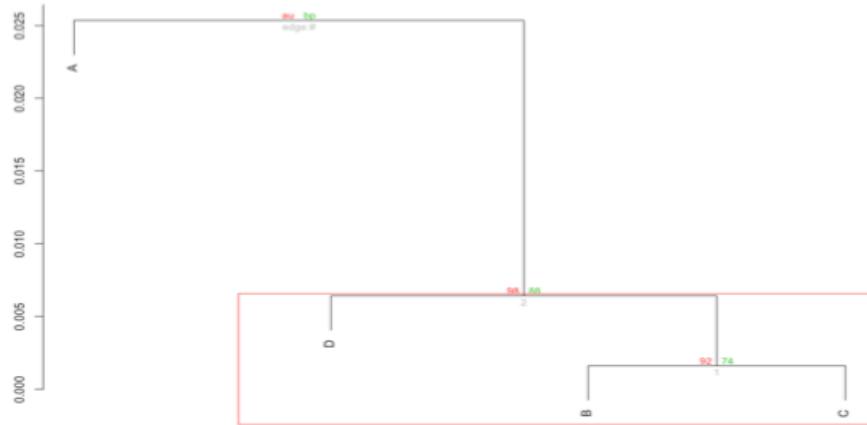


Figure 13. Hierarchical Clusters of Regular Firing Cells. Dendrograms showing the Euclidian distance between the means of each electrophysiological property for groups (Poly I:C), B (PLX), C (Wild Type), and D (Poly I:C and PLX).

RS EPSC PROPERTIES



RS IPSC PROPERTIES

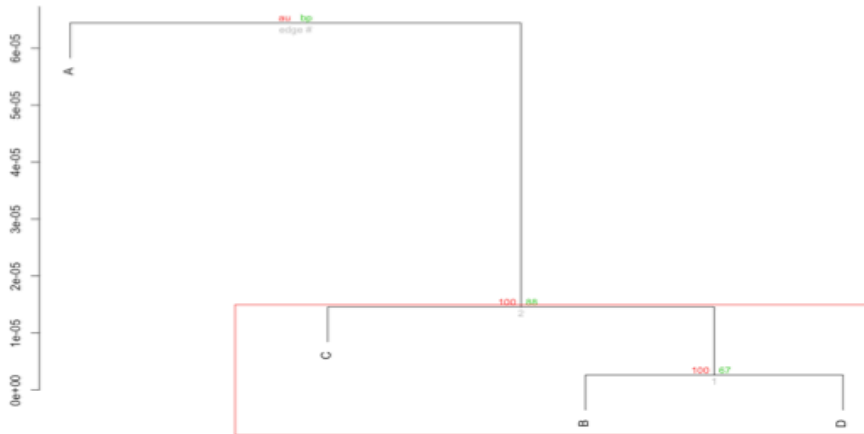


Figure 14. Hierarchical Clusters of Regular Firing Cells Synaptic Properties.

Dendrograms showing the Euclidian distance between the means of each electrophysiological property for groups (Poly I:C), B (PLX), C (Wild Type), and D (Poly I:C and PLX).

Behavioral Data between Groups

Behavioral Data was collected by the Ikezu Lab at the Boston University School of Medicine department of pharmacology. A sample of that data has been presented in this thesis in order to compare the behavioral profiles of the mouse models with their electrophysiological characteristics (Table 6). When compared to control (Saline) mice, Poly I:C mice were significantly different ($p < .05$) in five behavioral tests (Self-Grooming Test, % Marbles Buried, Open Field Moving Duration, Open Field Rotation Frequency, and Social Approach Preference Index). The PLX group was not significantly different than in all behavioral tests. An interaction between the effects of Poly I:C and PLX on control were observed in two behavioral tests (Self-Grooming Test and Social Approach Preference Index).

Table 6. Behavioral Data between Experimental Groups. Showing the average and standard deviation of each groups performance in behavioral tasks. Significant ANOVAs are shown in red. (Accredited to Maya Woodbury of the Ikeza Lab at the Boston University School of Medicine, unpublished)

Time	Behavior Test	Saline		Poly(I:C)		Saline + PLX		Poly(I:C) + PLX		1way ANOVA p-value	2way ANOVA			Summary
		AVG	STDEV	AVG	STDEV	AVG	STDEV	AVG	STDEV		Interaction	Poly(I:C)	PLX	
3 weeks old	Maternal Homing Test Preference Index (Mother vs. Empty Tube)	58.183	31.780	40.314	36.425	N/A	N/A	N/A	N/A	0.0085 (t-test)	N/A	N/A	N/A	Poly(I:C) decreases preference for mother vs. tube.
4 weeks old (1 st week of depletion)	Self-Grooming Test 1 Duration (s)	2.2742	1.2594	2.5717	0.9795	1.0133	0.6891	1.9271	1.2209	0.0058	0.3234	0.0036	0.0567	Poly(I:C) increases. PLX reduces.
5 weeks old (2 nd week of depletion)	% Marbles Buried	10.859	18.381	32.228	25.422	10.096	12.113	8.456	11.680	0.0014	0.0280	0.0340	0.0547	Poly(I:C) increases. PLX reduces only in Poly(I:C) mice.
6 weeks old (end of depletion)	Open Field Moving Duration (Center Pt)	500.398	32.468	528.290	16.946	496.784	33.932	505.422	40.962	0.0200	0.2348	0.0264	0.1041	Poly(I:C) increases. PLX no significant effect.
6 weeks old (end of depletion)	Open Field Rotation Frequency (Nose Pt)	28.875	7.830	33.684	9.534	23.615	6.838	31.500	14.119	0.0458	0.5482	0.0156	0.1492	Poly(I:C) increases. PLX no effect.
7 weeks old	Social Approach Preference Index (Social Chamber vs. Empty Chamber)	60.966	9.461	55.388	8.871	60.354	6.135	59.927	6.150	0.0280	0.0733	0.0406	0.7451	Poly(I:C) reduces social preference. PLX increases in Poly(I:C) only.

DISCUSSION

Electrophysiological of Experimental Groups

These results have overlying trends that are consistent with previously done research. They also have some discrepancies most likely due to the heterogeneity of the L5PNs. In terms of the electrophysiological parameters between RS, IB, and ROB neurons (Figures 5 and 6; Table 2), the RS and ROB neurons showed the most differences. IB neurons tended to fall between the other two types. This range of firing behaviors clearly demonstrates significantly different electrophysiological profiles. This is most likely due to the differential targeting that each of these neurons display. The IB and ROB types will be almost all subcortical, while RS cells can be both subcortical as well as cortico-cortical (Oswald *et al.*, 2013). Even though IB and RS cells show similar trends (Figures 11 through 14) when using their means in hierarchical clustering, the variation within the groups of the RS neurons overshadowed the significance between groups (Table 3). However, within the IB type, multiple significant differences were seen between the MIA group, and both the PLX and MIA/PLX groups (Table 5). The differences showed a consistent phenotype when relating MIA to PLX treatments, especially when looking at Rn, Vr, Rheobase, and Spike number at +100 mV. Compared to the control group, the MIA fired more quickly when injected with current, and are associated with hyper-excitability. The PLX group needed more current in order to fire, and was therefore less excitable than the control. This consistency across multiple

electrophysiological parameters allows for these phenotypical assumptions to have a strong base.

Something to consider is the wide range of electrophysiological profiles within the MIA model. On average, group A (Poly I:C) had the largest standard deviation within the IB database using all the intrinsic properties, and the second largest only to the Poly I:C and PLX treatment (group D) in the RS cells (Figures 7 and 8) (Table 3). While further analysis would be needed to infer anything statistically, the Poly I:C treatment does seem to result in a wide range of electrophysiological profiles. This phenomenon, however, isn't necessarily surprising. The Poly I:C is injected on embryonic day 9, which is very early in development. Also, this injection has an indiscriminant, but not necessarily consistent, effect on the cortex. The idea that each local circuit handles the MIA slightly differently depending on how many of the microglia are activated is by no means inconceivable.

An interesting contrast to the variety seen in the MIA model, is the consistency seen in the microglial depleted model (group B). In both RS and IB cells, group B had the smallest average standard deviation over all intrinsic properties. This, again, is not intuitively unsurprising. The PLX treatment has been shown to eliminate over 99 percent of microglia in the cortex, possibly leaving less inconsistencies. (Rice 2015) Also, important to note that the PLX treatment is given to mice 21 to 42 days after birth. Not only is this a very long time to deprive the juvenile mice of microglia, it also is much closer to the recording date than the administration of the MIA model.

The Effect of Diversity of Layer 5 Pyramidal Neurons on this Study

Intrinsic bursting is heavily, if not exclusively, associated with subcortical and thalamic pyramidal neurons with regard to layer 5 (Oswald *et al.*, 2013; Hattox *et al.*, 2007). Used as the primary criteria in order to split the neurons in for RS and IB groups should be consistent, though there is no way to verify this during the experiment. Another consideration is that one of the experimental groups could skew the firing type of target specific cells. Although this is not likely, it is important to note that R_n , which is related to rheobase, is higher in the MIA model, and lower in the microglial depletion model. Bursting properties have been shown to be effected by the temperature of the environment (Hendrick *et al.* 2011; Oswald *et al.* 2013). However, it is important to understand that the focus of this research is not to categorize normative data, but to measure the effects of the experimental models. In this respect the data regarding IB cells is much more consistent and substantive. They have similar morphological and physiological properties, and therefore, should be a good comparison across groups.

Consistent Patterns of Differences in Electrophysiological and Behavioral Profiles

This thesis covers the electrophysiological focus of a much larger MIA study done by the Tsuneya Ikezu lab (at Boston University School of Medicine Department of Pharmacology) in order to develop novel therapies for Autism Spectrum Disorder. In concurrence with the electrophysiological data collected there have also been behavioral

and morphological studies in order to build a profile of these experimental models. Maya Woodbury, a graduate student currently working on this project, was gracious enough to allow me to use the behavioral data collected in order to compare the results with the electrophysiological findings. In Table 6 there is a summary of the findings from the behavioral data. According to the table, Poly I:C mice behave significantly differently in comparison to the wild type mice, while there is no significant difference between PLX treated mice and wild type mice. The interactive group that received both Poly I:C and PLX behaved like the wild type in the self-grooming test, open field duration test, and open field rotation frequency, but different from the wild type in the marble burying test and the social approach test.

Because it is difficult to associate specific behavioral differences with electrophysiological properties, the best data to use in this comparison are the hierarchical cluster analyses (Figures 11 through 14). According to these similarity matrices, the PLX and Interaction groups behave the most similarly. The control group exhibited similarities with both the PLX/ Interaction group and the Poly I:C group, and the Poly i:C group is on the other end of the spectrum, furthest from PLX. Overall, these electrophysiological profiles are similar to the behavioral profile. The averages of the behavioral test show a polarization between the Poly I:C group and the PLX group, with the control averages being between them in every single test other than the social approach test. It can be inferred from this parallel presentation of data, that Poly I:C and PLX have polarizing effects on the mouse behavior and electrophysiology.

Conclusions

Despite some issues with pyramidal type targeting, conclusions can still be reached based on the data collected. As previously discussed, a more proactive labeling of target L5PN would decrease noise, allowing for a tighter baseline and less variation within groups. The inconsistency of the Poly I:C electrophysiological phenotype is also an issue in terms of separating its effect from the control. While it is apparent that the Poly I:C and PLX treatments exhibit opposing differences relative to the control group, the exact level of difference is hard to calculate. A more consistent method of inflammation, closer to the time of recording, is necessary to see the full effect of Poly I:C. This becomes even more apparent because of the consistency within the PLX and PLX/ Poly I:C treatment group. It is difficult to say if the strong effect seen was due to a lasting phenotype or whether it is due to of the proximity of recording to the drug being administered. If the PLX/ Poly I:C = group was given more time to recover after the PLX treatment, would its phenotype change in relationship to relative distance from the control and PLX group? Would it regress?

Exploring PLX further as a therapy for neuroinflammation does hold merit based on these findings. The PLX and PLX/Poly I:C groups did not differ significantly from control, and maintained a very strong and consistent phenotype. Only in one out of 8 hierarchical clusters did the means of these two groups *not* significantly cluster. Considering the variation within the RS group this is a strong result. Based on these

results there is a very good chance that the PLX treatment changes the phenotype of the Poly I:C mice into one that more closely resembles that of the PLX only treatment. Because the PLX only treatment does not significantly differ from control, and the vast majority of its characteristics are polarized when compared to Poly I:C it is possible that by decreasing the microglia, the PLX is indeed decreasing the effects of neuroinflammation.

Future Directions

Morphological analysis is an ongoing part of the study, and is not an explicit part of this thesis. Whole cell 40x confocal scanning and reconstruction of recorded and filled neurons, as can be seen in figure 3, will be used to study and compare the detailed dendritic morphology of these L5PN across four groups. In order to visualize the microglia, immunohistochemical co-labeled P2ry12 and IBA1 will be used to stain the microglia red. The goal is to count microglia and further assess their relationship with these pyramidal neurons. In addition, confocal scanning at high resolution of dendritic segments of these neurons will be used to count spines and assess their relationship with microglia. If we were to speculate, the associations established between the behavioral and electrophysiological data will likely also be consistent within the morphological data. Under this assumption, the Poly I:C and PLX treatments will have opposite effects on the neuronal anatomy. For example, if the Poly I:C model is found to have high spine density,

it would be reasonable to assume the PLX model will have decreased spine density. The unknown in this analysis would be dual-treated mice. Further analysis is needed to further phenotype this model. The data consistently shows that a PLX treatment after Poly I:C results in a change of both the behavioral and electrophysiological profile of the mice. While the shift away from the Poly I:C phenotype is very promising, the next step is to determine if this shift is towards the control, or is this dual drug administration being dragged into a phenotype that simply shares certain associations with both PLX and Poly I:C treatment. Hopefully the morphological analysis will further our understanding of this question.

REFERENCES

- Amatrudo, J.M., Weaver, C.M., Crimins, J.L., Hof, P.R., Rosene D.L., Luebke J.I. (2012) Influence of highly distinctive structural properties on the excitability of pyramidal neurons in monkey visual and prefrontal cortices *Journal of Neuroscience* 32(40), 13644–13660.
- American Psychiatric Association. (2013) *The Diagnostic and Statistical Manual of Mental Disorders*. 5th edition.
- Ashwood, P., Krakowiak, P., Hertz-Picciotto, I., Hansen, R., Pessah, I., & Van de Water, J. (2010) Elevated plasma cytokines in autism spectrum disorders provide evidence of immune dysfunction and are associated with impaired behavioral outcome. *Brain, Behavior, Immunity*, 25, 40-45.
- Atladóttir, H.Ó., Henriksen, T.B., Schendel, D.E., Parner, E.T. (2012) Autism after infection, febrile episodes, and antibiotic use during pregnancy: an exploratory study. *Pediatrics*, 130(6), 1447-54.
- Carper, R.A., & Courchesne, E. (2005) Localized enlargement of the frontal cortex in early autism. *Biological Psychiatry*, 57(2),126-33.
- Centers for Disease Control and Prevention. (2014) Retrieved from <http://www.cdc.gov/ncbddd/autism/>.
- Chez, M.G., Dowling, T., Patel, P.B., Khanna, P., & Kominsky, M. (2007) Elevation of tumor necrosis factor-alpha in cerebrospinal fluid of autistic children. *Pediatric Neurology*, 36(6), 361-5.
- Garay, P.A., Hsiao, E.Y., Patterson, P.H., & McAllister, A.K. (2013) Maternal immune activation causes age and region-specific changes in brain cytokines in offspring throughout development. *Brain, Behavior, Immunity*, 31, 54-68.
- Hattox, A.M., & Nelson, S.B. (2007) Layer V neurons in mouse cortex projecting to different targets have distinct physiological properties. *Journal of Neurophysiology*, 98(6), 3330-40.
- Hedrick, T. & Waters, J. (2011) Spiking patterns of neocortical L5 pyramidal neurons in vitro change with temperature. *Frontiers in Cellular Neuroscience*, 5, 1.
- Hustler, J. J. & H. Zhang. (2010) Increased dendritic spine densities on cortical projection neurons in autism spectrum disorders. *Brain Research*, 1309, 83-94.

- Kasper E.M., Lubke, J., Larkman, A.U., & Blakemore, C. (1994) Pyramidal neurons in layer 5 of the rat visual cortex. Differential maturation of axon targeting, dendritic morphology, and electrophysiological properties. *Journal of Comparative Neurology*, 339, 495–518.
- Lai, T., Jabaudon, D., Molyneaux, B.J., Azim, E., Arlotta, P., Menezes, J.R., & Macklis, J.D. (2008) SOX5 controls the sequential generation of distinct corticofugal neuron subtypes. *Neuron*, 57(2), 232-47.
- Malkova, N.V., Yu, C.Z., Hsiao, E.Y., Moore, M.J., & Patterson, P.H. (2012) Maternal immune activation yields offspring displaying mouse versions of the three core symptoms of autism. *Brain, Behavior, Immunity*, 26(4), 607-16.
- McKenna, W.L., Betancourt, J., Larkin, K.A., Abrams, B., Guo, C., Rubenstein, J.L., & Chen, B. (2011) Tbr1 and Fezf2 regulate alternate corticofugal neuronal identities during neocortical development. *Journal of Neuroscience*, 31(2), 549-64.
- Medalla, M. and Luebke, J.L. (2015) Diversity of glutamatergic synaptic strength in lateral prefrontal versus primary visual cortices in the rhesus monkey. *Journal of Neuroscience*, 35(1), 112-27.
- Molnár, Z., Cheung, A.F. (2006) Towards the classification of subpopulations of layer V pyramidal projection neurons. *Neuroscience Research*. 55(2), 105-15.
- Morgan, J.T., Chana, G., Pardo, C.A., Achim, C., Semendeferi, K., Buckwalter, J., Courchesne, & E., Everall, I.P. (2010) Microglial activation and increased microglial density observed in the dorsolateral prefrontal cortex in autism. *Biological Psychiatry*, 68(4), 368-76.
- Pellicano, E., Maybery, M., Durkin, K., & Maley, A. (2006) Multiple cognitive capabilities/deficits in children with an autism spectrum disorder: "weak" central coherence and its relationship to theory of mind and executive control. *Developmental Psychopathology*, 18(1), 77-98.
- Petanjek, Z., Judaš, M., Šimic, G., Rasin, M.R., Uylings, H.B., Rakic, P., & Kostovic, I. (2011) Extraordinary neoteny of synaptic spines in the human prefrontal cortex. *Proceedings of the National Academy of Sciences of the United States of America*, 108(32), 13281-6.

- Oswald, M.J., Tantirigama, M.L., Sonntag, I., Hughes, S.M., & Empson, R.M. (2013) Diversity of layer 5 projection neurons in the mouse motor cortex. *Frontiers of Cellular Neuroscience*, 7, 174.
- Rice, R.A., Spangenberg, E.E., Yamate-Morgan, H., Lee, R.J., Arora, R.P., Hernandez, M.X., Tenner, A.J., West, B.L., & Green, K.N. (2015) Elimination of Microglia Improves Functional Outcomes Following Extensive Neuronal Loss in the Hippocampus. *Journal of Neuroscience*, 35(27), 9977-89.
- Rossignol, D.A., & Frye, R.E. (2012) A review of research trends in physiological abnormalities in autism spectrum disorders: immune dysregulation, inflammation, oxidative stress, mitochondrial dysfunction and environmental toxicant exposures. *Molecular Psychiatry*, 17(4), 389-401.
- Schubert, D., Kötter, R., Luhmann, H.J., & Staiger, J.F. (2006) Morphology, electrophysiology and functional input connectivity of pyramidal neurons characterizes a genuine layer Va in the primary somatosensory cortex. *Cerebral Cortex*, 16(2), 223-36.
- Shai, A.S., Anastassiou, C.A., Larkum, M.E., & Koch, C. (2015) Physiology of layer 5 pyramidal neurons in mouse primary visual cortex: coincidence detection through bursting. *Public Library of Science Computational Biology*, 11(3).
- Silverman, J.L., Yang, M., Lord, C., & Crawley, J.N., (2010) Behavioural phenotyping assays for mouse models of autism. *Nature Review Neuroscience*, 11(7), 490-502.
- Soumiya, H., Fukumitsu, H., Furukawa, S., (2011) Prenatal immune challenge compromises development of upper-layer but not deeper-layer neurons of the mouse cerebral cortex. *Journal of Neuroscience*, 31(9), 1342-50.
- Suzuki, K., Sugihara, G., Ouchi, Y., Nakamura, K., Futatsubashi, M., Takebayashi, K., Yoshihara, Y., Omata, K., Matsumoto, K., Tsuchiya, K.J., Iwata, Y., Tsujii, M., Sugiyama, T., & Mori, N. (2013) Microglial activation in young adults with autism spectrum disorder. *JAMA Psychiatry*, 70(1), 49-58.
- Tantirigama, M.L., Oswald, M.J., Clare, A.J., Wicky, H.E., Day, R.C., Hughes, S.M., & Empson, R.M. (2016) Fezf2 expression in layer 5 projection neurons of mature mouse motor cortex. *Journal of Computational Neurology*, 524(4), 829-45.

- Willsey, A.J., Sanders, S.J., Li, M., Dong, S., Tebbenkamp, A.T., Muhle, R.A., Reilly, S.K., Lin, L., Fertuzinhos, S., Miller, J.A., Murtha, M.T., Bichsel, C., Niu, W., Cotney, J., Ercan-Sencicek, A.G., Gockley, J., Gupta, A.R., Han, W., He, X., Hoffman, E.J., Klei, L., Lei, J., Liu, W., Liu, L., Lu, C., Xu, X., Zhu, Y., Mane, S.M., Lein, E.S., Wei, L., Noonan, J.P., Roeder, K., Devlin, B., Sestan, N., & State, M.W. (2013) Coexpression networks implicate human midfetal deep cortical projection neurons in the pathogenesis of autism. *Cell*, 155(5), 997-1007.
- Yang, C.R., Seamans J.K., & Gorelova N. (1996) Electrophysiological and morphological properties of layers V-VI principal pyramidal cells in rat prefrontal cortex in vitro. *Journal of Neuroscience*, 1 March 1996, 16(5): 1904-1921;
- Zhan, Y., Paolicelli, R.C., Sforzini, F., Weinhard, L., Bolasco, G., Pagani, F., Vyssotski, A.L., Bifone, A., Gozzi, A., Ragozzino, D., & Gross, C.T. (2014) Deficient neuron-microglia signaling results in impaired functional brain connectivity and social behavior. *Nature Neuroscience*, 17(3), 400-6.

CURRICULUM VITAE

CARL SEILIER HOLLAND III

Year of Birth: 1990
233 Northampton Street, Apt. 3
Boston MA, 02118
(904) 535-5739
carlholland09@gmail.com

Education

Bachelors of Arts in Neuroscience from Johns Hopkins University- Baltimore Maryland
(August 2009 though May 2013)

Candidate for a Masters in Science in Anatomy and Neurobiology from Boston
University Medical School- Boston, Massachusetts (August 2014- present)

Research Experience

Trainee as a Lab Tech in Ferenc Deak's Electrophysiology Lab, Mayo Clinic (Summer 2010)

- Basic lab tech duties: Mixing solutions, measuring and handling dangerous chemicals, splicing and cloning viral vectors, growing and maintaining cell lines, dissection of live mouse brain while maintaining health of neurons, and preparing samples for fluorescent imaging and patch clamp experiments.
- Over 120 hours of experience in the lab in the summer of 2010, used for school research credit at Johns Hopkins University.

Trainee as a Research Assistant in Ferenc Deak's Electrophysiology Lab, Mayo Clinic (Summer 2011)

- Research Assistant Duties: Preparing and Running Fluorescent Imaging Experiments and collecting data, Prepping and Running Multi-Electrode array experiments and collecting data, Dissecting and preparing mouse hippocampal slices for Multi-Electrode Array Experiments, basic data analysis
- Details on research: The fluorescent imaging studies were used to determine the role of Synaptobrevin 1 compared to the better know effects of Synaptobrevin 2 on the efficiency of the SNARE complex and its role in vesicle fusion, exocytosis, and recycling. The Multi Electrode Array studies were used to study the changes

in long-term potentiation in the tract between CA3 and CA1 in the hippocampus within LRP6 deficient mice compared to wild type mice.

- Over 120 hours of experience in the lab in the summer of 2011, used for school research credit at Johns Hopkins University.

Scientific lab courses completed at Johns Hopkins

- The lab work I completed at Johns Hopkins also should be noted as it demonstrates the wide range of lab techniques I've accumulated in my academic career. They are as follows: General Physics Lab I and II, General Biology Lab I and II, Organic Chemistry Lab, Biochemistry Lab, Cell Biology Lab, and Neuroscience Lab (Anatomy and Electrophysiology concentration)

Work experience and Community Service

Tutor (2010-2012, 4 semesters) and Organizer (2012-2013, 2 semesters) in the Johns Hopkins Tutorial Project

- Duties as a tutor: 4 hours a week commitment to the program tutoring a child from public elementary school from Baltimore City. Most of these children had either academic or behavioral difficulties, and benefited greatly from studying with students from Johns Hopkins.
- Duties as an organizer: Organizer is a leadership position within the Tutorial project selected from a pool of applicants. As an organizer I was accountable for six pairs tutor-tutee pairs among many other responsibilities. Other than monitoring week to week academic and behavioral progress of the pairs, I was also in charge of the students testing, the tutors teaching methods, safety of the tutees on the Johns Hopkins campus, as well as keeping the parents informed of their children's progress with written reports and necessary disciplinary phone calls. These duties accumulated to around 8 to 10 hours a week.

Tutor for Jail Tutorial Project (freshman year, 1 semester)

- Duties as a tutor: Commuting to and from the Maryland Metropolitan Transition Center in downtown Baltimore to tutor female inmates attempting to receive their GED. The inmates were in a special program allowing them to study, and be tutored by Johns Hopkins students in high school level math and English. This program had a 5 hour a week commitment.

Alumni Chair for Sigma Phi Epsilon Fraternity (Junior Year, 2 semesters)

- Duties included by-monthly meetings with the alumni board in order to report on the development of alumni affairs and donations. Coordination with Alumni to update them on the current state of the fraternity.

Camp Counselor (Counselor in Training Program, summer 08 and Assistant Counselor, summer 09)

- Full time employee of the Camp High Rocks summer camp for boys. Duties included taking care of and being responsible for a cabin of eight campers and developing their social and outdoor skills. I learned both important leadership development, and team building exercises, in both teaching the campers, and working with other counselors, over four months in the mountains of North Carolina.

Relevant Skills

- Proficient in multi-electrode array recording, fluorescent imaging recording, preparation of solutions, maintaining cell lines, slicing and preparing mouse hippocampal slices, tutoring math and English, Microsoft PowerPoint, Microsoft Excel
- Background in patch clamp recording, splicing and cloning viral vectors, maintaining cell lines, analyzing electrophysiology (patch clamp, fluorescent imaging, and multi-electrode array) recordings, SPSS, NeuronStudio,